2D nanomaterials for Energy Storage

Sufyan Naseer **Registration. No. NUST201435037BCSME99214F**

Qaisar Abbas **Registration. No. NUST201434960BCSME99214F**

Khalid Mansoor **Registration. No. NUST201432796BCSME99214F**

This report is submitted as a FYP thesis in partial fulfillment of the requirement for the degree of (BE in Materials Engineering)

Supervisor: Dr. Sofia Javed

Department of Materials Engineering

School of Chemical and Materials Engineering

National University of Sciences and Technology

2018

Certificate

This is to certify that the work in this thesis has been carried out by Qaisar Abbas, Khalid Mansoor and Sufyan Naseer, and completed under my supervision in Nano Synthesis Laboratory, School of Chemical and Materials Engineering, National University of Sciences and Technology, H-12, Islamabad, Pakistan.

Supervisor: Dr. Sofia Javed

_____

Department of Materials Engineering
School of Chemical & Materials Engineering,
National University of Sciences and Technology, Islamabad

Submitted through:

HoD**:** _____
Department of Materials Engineering
School of Chemical & Materials Engineering,
National University of Sciences and Technology, Islamabad

Dean**:** _____
Department of Materials Engineering
School of Chemical & Materials Engineering,
National University of Sciences and Technology, Islamabad

Dedication:

This thesis is dedicated to all the faculty members of department of Materials Engineering, School of Chemical and Materials Engineering, National University of Sciences and Technology.

It is also dedicated to our supervisor for her continuous support throughout the project, and to our fellow research groups.

Acknowledgement:

We wish to express our sincere thanks to the administration of School of Chemical and Materials Engineering for providing us with all the necessary facilities for the research.

We are also grateful to our project supervisor **Dr. Sofia Javed** for guiding us throughout this project and sharing with us the valuable knowledge and expertise needed for this project.

We take this opportunity to express our gratitude to all of the Department faculty members for their help and support. We also thank senior research fellows for their continuous encouragement and support.

We also place on record, our sense of gratitude to one and all, who directly or indirectly, have lent their hand in this venture.

Abstract:

Our aim is to develop ultrathin 2D-nanomaterials which can be used for energy storage and photo-catalysis. The most popular candidate for this purpose is graphene Nano-sheets, which are obtained from graphite by chemical exfoliation method. The application of graphene in the field of electrochemical energy storage devices has been extensively investigated due to its many promising physical and chemical properties. Graphene is a flat monolayer of carbon atoms with perfect sp-hybridized two- dimensional carbon structure. It has high conductivity, superior electron mobility, extremely high specific surface area, excellent optical transmittance and easy functionalization makes graphene a good substrate to produce graphene based composites for energy storage. Especially, graphene – Metal Chalcogenides (e.g. WS_2, MoS_2, etc.) composites that have attracted extensive attention for their potential applications in energy related areas.

List of Figures

List of Tables

Table of Content

Chapter 1: Introduction

Materials science is traditionally based on two vertices, structure and processing bridging with the properties and performance. Processing materials into desired structure by enabling the controlled synthesis of materials to form thin layers and various hierarchical architecture, to discover the properties for many practical applications.

1.1 Energy Crisis

Energy is essential for the growth of the economy. Currently, the main source for the fulfillment of our energy needs are fossil fuels, and this has been the case ever since the industrial revolution. The ever rising world population (doubled in the past 40 years from 3.7 billion to the present 7 billion) is leading to rising demand for energy, while our fossil fuel reserves are limited. By 2030, a further rise to more than 8 billion people is expected. Another reason for the ever-rising demand is the rising standards of living. The primary energy demand in Germany is ≈ 45 000 kWh/head; in a developing country such as Bangladesh, however, it's just 1500 kWh/head. As the standards of living rise, these figures go up considerably. China, being a strong growing economy, has the need of over 16 000 kWh/ head. The International Energy Agency (IEA) expects that China's energy requirement in the next 25 years will rise by 75% and India's by 100%.

The worldwide requirement for energy is covered today mainly by the fossil fuels: oil, natural gas and coal. They make up a portion of more than 80%, whilst biomass, hydro and renewable energies (wind, photovoltaics, solar heat, etc.) up till now have only reached 10%. Meanwhile, the strong usage of fossil sources has led to scarcity. In 2001 the reserves of oil were estimated to last 43 years and natural gas 64 years. Only coal reserves were estimated to last for a relatively long period of 215 years. If one assumes that the world energy consumption continues to grow as previously, then reserves will be reduced drastically in 30 – 65 years. The scarcity of fuels will lead to strongly rising prices and distribution wars. Previously, oil

extraction from oil sands and oil shales has also been done, especially in Canada and the USA. The production of synthetic oil, as such, requires too much work to be feasible. Also, this extraction causes the destruction of otherwise undisturbed ecosystems. So, turning towards alternative fossil resources is really not an option as of yet.

Decomposing biomass (plants, wood etc.) releases CO_2 into the atmosphere. Growing plants take up CO_2 from the air, for photosynthesis. In non-industrialized times, the uptake and release of CO_2 was cancelled out and there was no problem of too much excess CO_2 in the air. When we burn wood as a source of energy, CO_2 is released. However, if we assume that all trees cut for firewood are replaced by new ones (as is the law in most countries), then we can also assume that as a result, the CO_2 that was released by burning the trees has been taken up by the new trees (for photosynthesis). On the other hand, when we talk about fossil fuels like coal, oil, and natural gas, the story is very different. Fossil fuels were formed over millions of years and are being used up in around 2 centuries, more or less. If we study the concentration of CO_2 in the atmosphere, we can find that even though there were variations even in the past, but the real alarming increase comes after the start of industrialization. In 2012, the CO_2 concentration was ≈ 400 ppm, which hasn't been seen in millions of years.

1.2 Energy Storage Media

Utilization of fossil fuels to meet the energy requirements of the world has an immense adverse impact on the environment. Due to these factors and many more besides, we must look for feasible alternative energy sources and implement them as soon as possible. Alternative energy sources include those that are renewable and environmentally clean, e.g. solar power, hydrogen-based energy, biofuel, wind, hydropower, and geothermal energy. To make alternative energy a key player in the international energy supply, we must first solve two important problems: we must raise the efficiency of energy generation to the point that it becomes equivalent to the current supply's efficiency (if not better). Secondly, energy storage devices of a high performance capability and low weight must be designed

and put in use, so that the problems of portability and the discontinuous nature of wind and solar energy, are solved.

Over the last few years, lithium-ion batteries have emerged as one of the most promising energy storage devices due to their high energy density storage capacity. Li-ion batteries are widely used in portable electronics; and currently, numerous research efforts are focused on their large-scale implementation in hybrid and pure electric vehicles. However, these large-scale transportation applications are primarily hindered by performance, safety, and cost of the electrode, electrolyte materials, and other battery components.

As advanced energy systems with enhanced conversion efficiencies, improved storage capacities, and better reliabilities are being developed to meet the global energy needs of the world's growing population, these aspects have emerged key factors that affect the performance of energy materials. Energy storage is the capture of energy produced at one time for use at a later time. A device that stores energy is sometimes called an accumulator. Energy comes in multiple forms including radiation, chemical, gravitational potential, electrical potential, electricity, elevated temperature, latent heat and kinetic. Energy other form of Bioenergy storage involves converting energy from forms that are difficult to store to more conveniently or economically storable forms. Bulk energy storage is dominated by pumped hydro, which accounts for 99% of global energy storage.

1.3 Materials for Energy Storage

High temperature & Cryogenic Materials:

Balancing the time difference between the supply and demand for power, can be done by a method known as Thermal Energy Storage. Residual or surplus heat is stored in the material as "sensible" or "latent" heat, by increasing the temperature, or changing the state (melting) of the material. This can be used up later, by decreasing the temperature of the material again. Thermal energy storage can also be used (potentially) for energy recovery (heat exchanger), using solar energy, reducing the energy consumption in buildings, and electronic device management.

Thin-film/3-D batteries for micro-electronics

Thin-film batteries are hypothesized to have superiority over conventional batteries in many ways. The thin-film batteries are made as thin (e.g. 1 micron) sheets that are stacked on top of each other, using methods that are currently used to make electronics, adjusted according to the application. Lithographic methods can be used to change the sheet area, from achieved size to several meter sq., thus broadening the collection of battery capacities that can be achieved. The thin-films mean that the anode and cathode are close together, thus allowing high current density and cell efficiency, and also reducing the reactant quantity that is needed. The reason being that ions can be transported faster and more easily in thin films because the distance to be traveled is less. The most important thing in the performance of the battery is the electrolyte that is chosen for it. It is a well-known fact that the main cause of limiting the recharge ability of old batteries is that their electrolytes have failed. The reason that batteries fail after some number of cycles (charge/discharge) and them losing charge is that the anode and electrolyte react. For example, in lithium-ion batteries, the lithium anode attacks the lithium electrolyte. Applying a protective layer on the surface of the anode, in the form of a coat, makes the battery larger and more complex, as well as expensive. The cathode determines the power and energy density of the battery. We need to keep the open circuit voltage and the current density at the time of discharge high, so that we can get the best performance out of it. Also, to this end, the rate of recharge should be high as well. The battery needs to be capable of withstanding a large number of cycles with little to no drop in its performance. [1]

Lithium and sodium sulfur batteries

Rechargeable lithium-ion batteries (LIBs) are now the main type of energy storage device for all mobile uses. The reason for this is that the energy density of LIBs is unmatched, being much higher than other batteries such as lead acid batteries. This notwithstanding, we require safer means of storing energy, as well as smaller devices that are less costly. For this, research is ongoing. Also a major problem is the requirement for cheap stationary energy storing. Much research has been done on the improvement of existing Li-ion technology, and resultantly, we have achieved higher efficiency in processing and packaging as well as superior

electrolytes and electrode materials. The power density has been improved considerably in recent years, but energy density has proven hard to improve.[2]

Organic batteries and Photovoltaics

Recently, organic-based photovoltaics have been given a boost in terms of research in that they have become widely pursued in research carried out by industries, as compared to before, when the research was limited to basics at the university laboratory level. The reason for this is that their efficiency of power conversion has risen considerably. The ease of manufacture of organic photovoltaics (made from polymers etc.) as compared to those made from silicon etc. also make them highly desirable. We could potentially cover a considerable amount of our requirements for energy if we started widespread production of organic based photovoltaics (to make them sustainable). The detrimental effect on the environment would be next to nothing, as compared to other energy storage methods. The only negatives would be the starting energy that is needed for device manufacture (included in their cost), waste materials from the production process (also very little) and the land area needed to install the organic photovoltaic assemblies. A photovoltaic device, converts absorbed photons directly into electrical charges that are used to energize an external circuit. The efficiency of power conversion of the photovoltaic process (direct conversion of absorbed photons into electric charge) is defined as the ratio of the electric power that we provide to the external circuit, to the solar power incident on the active area of the device. Efficiencies of over 24% have been achieved for such devices in the laboratory. [3]

Large Scale Grid Storage

Electrical energy storage (EES) is a widely-recognized method for upgrading grid reliability as well as utilization. Transporting electricity from place to place is done using transmission and distribution networks. The EES incorporate a time dimension into the equation; they supply energy when it is required. Recently, studies have shown a few valuable applications for this type of energy storage: from the incorporation of renewable power to quality and reliability of power. Even though the potential advantages are numerous and highly desirable, there are very

few storage systems in operation in the USA and around the world. The power supplied in the USA has a small fraction of ≈ 2.5 % that utilizes energy storage. The types of energy storage that can be applied to widespread use are: chemical, mechanical, electrochemical, and electrical. 99 % of the global storage capacity is accounted for by pumped hydroelectric systems. This equates to around 127,000 MW of output power. In second place, compressed air storage accounts for a paltry 440 MW. The possibilities for EES in the grid include regulation of frequency, peak shaving, load following, and load shifting. Peak shaving and load shifting result in increases in reliability, grid stability and cost. When surplus power is generated, load shifting can store this energy and supply it when it is required. That being said, the technical demands for such a system are very difficult to overcome. EES storage has a few major advantages: the capability to be operated pollution-free, high efficiency, adjustable power characteristics and energy characteristics for varying grid requirements, long life, and minimal maintenance.[4]

Supercapacitors.

Batteries have the capability to allow the devices that run on them running through entire days. This means that their energy density is very high. However, when we have to charge them up again, it takes quite some time (up to a few hours). We can rephrase this by saying that their power density is low. To increase power density, meaning fast delivery of power (in a burst) and fast charging, we can use supercapacitors. That said, their energy density is low. [5]

Double-layer capacitance:

The interfacial specific double-layer capacitance at electrode surfaces is normally (to a considerable extent) dependent on electrode potential and the physicochemical characteristics of the electrode surface (especially regarding carbon materials, contingent upon their origin, conditioning treatment and the degree to which they have been graphitized). The "reference example" is normally the mercury/solution interface, the double-layer capacitance of which differs considerably through the potential of zero (surface) charge densities and is largely conditional on the character of the electrolyte's anions which can be adsorbed at Hg, and on the dipolar

character, the solvent's electron-donor number, and its solvating power for anions and cations of the electrolyte solute.

At solid, especially noble, metals, again the double-layer capacitance is, to a considerable degree, dependent on the metal's identity and mainly whether the metal has a thin oxide coating (e.g. Pt or Au) and at which single-crystal electrode surface plane, e.g. Au, we measure the capacitance. At such electrodes, the point of zero charge is particular to the surface plane's Miller index orientation and is directly related to the electron work-function of said plane.

The idea is of a capacitor device, making use of the interfacial double-layer capacitance of a poriferous electrode structure having a large surface area. Nonetheless, the initial prototype was quite basic and insufficiently described, causing later misconceptions of the dissimilarity of the functions of electrochemical capacitors and faradaic battery systems. A carbon double-layer capacitor working in a non-aqueous, aprotic solvent such as propylene carbonate containing a tetraalkylammonium salt as electrolyte, allows a considerably higher voltage of 3.5 V on charge to be achieved with a correspondingly higher energy density of ≈ 8.5 times that for an aqueous system where the thermodynamic maximum voltage on charge is the decomposition potential of water, 1.23 V. Capacitors have energy density equal to qV (CV^2); q being the charge density when the voltage is equal to V. In comparison, the cell of a battery has energy density qV (using the same values of q and V), which is double that for a capacitor under the same conditions.

Pseudo capacitors:

Initially, when interest in supercapacitor development was piqued (around 1990) e.g.by the initiation of the Florida Educational Seminar Series on Double-Layer Capacitors and Related Devices in 1991, we did not understand the difference between pseudo-capacitance and double-layer capacitance very well. However, in basic electrochemistry it was a widespread concept much earlier and a central bridging paper was that, in which it was acknowledged that the cyclic voltammetry trends of RuO_2 DSA electrodes, produced as stable anodes for industrial Cl_2 production, had the formation equivalent to a capacitor under linear voltage sweep modulation. Pseudo-capacitance, related with the under-potential deposition of

adatoms of Hydrogen (and subsequently, of metal atoms), was also covered in depth by Conway and Gileadi (Researchers) earlier. When the charge (q) passed, e.g. in an electrosorption process or in a quasi-two-dimensional intercalation process, or in a surface redox process as with RuO_2, is a function of electrode potential, then a derivative, dq/dV, can be used that shows capacitance and can be used to measure it. This capacitance is of faradaic origin, instead of being related to potential-dependent increase of electrostatic charge, as is the case in a double layer, relating to double-layer capacitance; therefore it is known as pseudocapacitance, the charging of which is faradaic.

Double-layer capacitance	**Pseudocapacitance**
Non-faradaic	Involves faradaic process
20–50 μF cm^{-2}	2000 μF cm^{-2} for single-state process; 200–500 μF cm^{-2} for multi-state, overlapping processes
C fairly constant with potential	*C* fairly constant with potential for RuO_2
Highly reversible charging/discharging	Quite reversible but has intrinsic electrode-kinetic rate limitation determined by R_f
Has restricted voltage range	Has restricted voltage range
Exhibits mirror-image voltammograms	Exhibits mirror-image voltammograms

Table: Comparison between Double-Layer and Pseudocapacitance.

Novel materials for enhanced battery performance

LiFePO4 has been suggested as a material to be used as the cathode in Li-ion batteries. It is of greater significance as compared to the other materials that are currently being researched for the same purpose. This is because of its inexpensiveness and the fact that its components are environmentally compatible. However, the LiFePO4 cathode experiences reduction in capacity as the current density increases. This specific cathode material has a specific capacity

(theoretical) of 170 mAhg-1. It has a low rate (5micro-amperes) of charge and discharge, and in reality, the capacity is actually lesser in the region of 120 $mAhg^{-1}$. [6]

1.4 Materials for Supercapacitors

Scientists and researchers has created a double-layer capacitor from carbonaceous materials (e.g., coconut shells, wood flour, coal, resin). This is done by using an alkali-metal hydroxide bath to heat-treat an active carbon precursor at 700°C. Specific capacitance of 500 F/g at the highest was obtained and surface area values ranged approximately 1000-1500 m^2/g.

Another capacitor was made with one electrode made up of a carbonaceous material and the other from an inorganic redox material comprising Ru, Rh, Pd, Os, Ir, Co Ni, Mn, Pt, Fe, alloys of Ru, Rh, Pd, Os, Ir, Co, Ni, Fe, Pt, oxide of Ru, Rh, Pd, Os, Ir, Co, Ni, Mn, Fe, and Pt, and combinations thereof. Activated carbon with a capacity of 2.7 F/g with a cobalt oxide counter electrode showed an effective voltage range of 1.8 V.

Other research projects on the basis of supercapacitors include:

- Pseudo capacitance with a multiphase anode material having the formula TMOiXC where TM = V, Zr, Hf, Ti, Nb, Sc, and combinations thereof. O = oxygen, X =modifier element: F, Cl, Br, I, and a = 0.1 to 3; 6 = 1 to 7, and c = 0 to 5.[7]
- Rechargeable energy storage device with electrodes made of organometallic compound selected from the group consisting of metallocenes, metal porphyrins, metal acetyl-acetonates, organometallic polymers, and metal di-pyridines blended or coated. Cobalt acetate-based electrodes showed a voltage of 0.725 V after charging. [7]
- Electrode material is a mixed valence complex (e.g., platinum blues, platinum reds, cis-diamine platinum alpha-pyridine blue, tetracyano-platinate complexes with stacked anions) containing at least two metal atoms and at least one ligand attached to the metal atoms, the metals exist in multiple oxidation states.[7]

- Activated carbon (>50%)/polyene composite containing Au, Pt, C, TiN, TiC showed low equivalent series resistance of 0.02 to 0.03 W at capacitances of 2.5 F
- Carbon foam electrode made by pyrolysis of resorcinol-formaldehyde and related polymers to realize high surface area electrode areas (400 to 1,000 mi/g) and capacities of 15 to 16 F/g.[7]
- Double-layer capacitor with electrodes comprised of a crystalline material (e.g., bismuth chalcogenides, BiTe3, Bi2Se3) with van der Waals channels showed capacities of 30 to 100 F/cm3 over 2.6 V in LiCIO4 solutions.[7]
- Double-layer capacitor comprising a conductive solid in contact with an inert gas to achieve high specific energy density.[7]
- High surface area carbon electrode (>1,000 m3/g) formed from filler particles having a high surface to volume ratio.[7]

Characteristic Properties:

Electrode materials necessitate high specific double layer capacitance or high specific pseudo capacitance. We must tailor the electrode to the high frequency response for fast charge/discharge performance by properly utilizing active materials.

A central factor in increasing capacitance is the electrode surface area. Other factors include good conduction of electricity, being electrochemically inert, as well as having low weight.

The large capacitance increases are due to the combination of a very small distance separating the opposite charges, as defined by the electric double-layer; and very porous electrodes having high surface-area. Porous carbon is preferred in various forms as an electrode material because it has very high surface area, comparatively high electronic conductivity, and reasonable cost.

The capability of the capacitor device to store energy is related to the physical and chemical properties of its electrodes. For instance, increasing the specific surface area, by activating carbon, usually results in a capacitance increase. The surface area in contact with the electrolyte is the only surface area contributing to

capacitance, carbon activation is needed to create open pores, connecting to the pore network. Even though the modern day supercapacitors have high performances, there is a lot of room to improve and make these figures even better. For example, there is significant opportunity to make the high frequency performance better. So, we can deduce that carbon will keep playing a central part in supercapacitors, by improving porosity, improving wettability through treatment of surfaces, and decreasing the inter-particle contact resistance.

The electrode materials for supercapacitors must have a singular collection of properties (both chemical as well as physical), including: high conductivity, high surface-area range (~1 to >2000 $m^2 g^{-1}$), good corrosion resistance, high temperature stability, controlled pore structure, process-ability and compatibility in composite materials and comparative cheapness.[8]

Examples:

- Neural and cardiac stimulating electrodes which are required to inject up to 10 mC/cm^2 within 200 μs intervals without any irreversible faradaic reactions such as gas evolution or metal dissolution summary of the maximum injectable charge for some materials.
- S/S^{2-} system with 6 M Na_2S in LiCl-KCl melt at 400°C which showed 2-5 mF/cm^2. Of all these C® based compositions, the only material that has been commercialized is RuO_2. EC systems based on RuO_2 show high specific capacitance because of the C® arising from the surface reaction.

$$2RuO_2 + 2H^+ + 2e^- = Ru_20_3 + H_20$$

Maximum capacitances of 2.8 F/cm2 were found with compositions based on RuO_2, mixtures of RuO_2 and Ta_2O_5 and mixed oxides of Mo, W, Co, and Ni. 30 RuO_2 bonded solid ionomer membranes showed 6-10 F/gm of active materials with very good charge-density delivery in pulse applications.

The evidently better performance of the RuO_2-based ECs is a result of the high i_0 of the RuO_2/Ru_2O_3 reaction, but this benefit is cancelled by the porosity of the RuO_2 matrix used in the EC device. Expectations of superior performance can only be had of thin RuO_2 films, since the matrix resistivity of thick electrodes will cancel out the advantages of the high intrinsic i_0 of the Ru02/Ru203 system. Note that the

magnitude of $C_{®}$ can be as large as 8F/cm2. Based on the definition of $C_{®,}$ with I_o mol/cm^2, n = 2, and a surface roughness factor of 100. Electrodes with such low roughness can be regarded as nearly planar, extended area electrodes. Enhanced $C_{®}$ + C_d via increased voltage domain.

1.5 Heterogeneous Nanomaterials and nanocomposites

Heterostructured nanomaterials, which may have superior electrochemical properties than single layered structure materials. Can be synthesized as the three-dimensional (2D) multicomponent oxide. Hierarchical heterostructures that are well prepared by refluxing technique under normal conditions, surface modification can be attained. To fabricated an asymmetric supercapacitor based on hierarchical heterostructured nanosheets, which can shown a specific capacitance of 187.1 F g^{-1} at current density of 1 A g^{-1}, and good reversibility with a cyclic efficiency of 98% after 1,000 cycles. These results indicates that forming a 2D hierarchical heterostructures can improve electrochemical properties. [9]

An example of ZnO/Au heterostructured nanoparticles also give favorable results when This can be constructed through epitaxial growth of Au on the ZnO seeds. The structure and morphology of ZnO/Au nanocomposites are investigated by TEM and XRD analysis. The ZnO/Au nanocomposite exhibits a strong absorption in the visible region and Ultra Violet regions. The band gap of n-type ZnO lie within the range of 4.2-5.8 eV, and for intrinsic ZnO it should be 5.3 eV. So, Au with 5.1 eV can donate electrons to ZnO.

Super capacitors, the range of topics will include capacitor performances for power uses such as electric vehicles, energy back-up applications, and renewable energy storage systems. Materials (such as, including but not limited to carbonaceous materials, intercalation compounds, metal oxides, nitrides, molybdates, phosphates, polymers and other composites) for electrochemical double layer, hybrid, redox, symmetric and asymmetric capacitor systems will also be included. The choice of materials is having a wide range from oxide materials to recently synthesized transition metal di- chalcogenides and dimension-wise they can be in bulk, surface, monolayer phase or in form of hetero- structures and nano-composites.

In the present age, one of our biggest problems is that how to cost and labor-effectively store energy. Two of the biggest ways of doing this are: using batteries and supercapacitors. These have attracted attention from all around the world due to the fact that they have become indispensable in our daily lives. These are the main source of power for all of our electronic devices e.g. our phones and computers. We can now power vehicles by electrical energy. Supercapacitors and Batteries basically belongs to the electrochemical devices although they have remarkably different meanings. They have resemblance in terms of their configurational and organizational structure. An integrated Lithium Ion Batteries (LIB) / Super Capacitors (SC) system consists of three components: a positive electrode (cathode), an electrolyte and a negative electrode (anode).

On charge, cations and anions travel from an electrode/electrolyte to the other and then get attached to it, resulting high polarization of the system. In Discharging process ions extract themselves spontaneously from electrode's surface and go back to other. During this whole process electrons continuously moves around the circuit.

LIBs and SCs have different charge storage processes. SCs are of two types: electric double layer capacitors (EDLCs) and pseudo-capacitors. Both these two types store charge only on their surfaces or in a very thin layer of active material by the process of absorption/desorption of ions to form electric double layers or using reversible surface/near-surface Faradic reactions. By this method, SCs can provide high charge/discharge capabilities and therefore they have very high-power densities. This is due to their non-solid ion diffusion while possessing poor energy density caused by limited active surface areas for (EDLCs), or inadequate use of entire pseudo capacitive materials (for pseudo capacitors).The high efficiency necessitates that the equipment be capable of storing high amounts of electrical energy in minimal space and then to transmit it very quickly. This could not have been possible without a logical and reasoned scheme for the suitable electrode materials.

Chapter 2: 2D Nano Materials

Nanomaterials, and specifically often metal oxides, have been under investigation as potential electrode materials for LIBs and pseudo capacitors due to the comparative effortlessness required in their mass production. Another reason is their rich redox reactions of different ions, which results in high specific capacities/capacitances.

Transition metal oxides are especially fascinating in the regard of their usefulness and their ability to store Li using the conversion method. Some metal oxides such as iron and manganese oxides are easily found in nature, they are plentiful and cheap. Additionally, the size, form, structure and orientation of metal oxide nanostructures can be straightforwardly adjusted to specific considerations. This makes it feasible to explore the structure-electrochemical property relationships. On the other hand, usage of metal oxides can also be disadvantageous. Most of the widely-studied oxides such as Manganese oxide, Nitrogen oxide etc., are wide bandgap semiconductors or sometimes insulators. This means that they manifest mediocre electrical conductivity. This is quite undesirable, because this can cause safety issues due to high production of heat energy as a byproduct of the charging and discharging.

Another point is that metal oxides have poor ion transport kinetics. Downscaling these oxides into nanoscale size or making hierarchically porous structures to ease the passage of ions in entering the inner side of the electrode matrix by providing enough ion transport pathways. Simultaneously, this causes an increase in the electrical resistance in the solid electrode because it has a higher number of grain boundaries.

Nanostructured materials are analyzed and classified on the basis of dimensionality of the nanostructure and their components. Nanostructure classification is suggested from build to form the constituting fundamental units, name as, 0D (clusters and particles), 1D (nanotubes and nanowires), 2D (nanoplates and layers).

Different nanostructure's size factors enabled us to predict qualitatively the properties of nanostructured materials and their applications in Nano devices. [10]

The materials we have pursued in our project are 2D nanomaterials for energy storage.

Investigation of Nano architectonics in 2D has made a great progress these days. Essentially, 2D nanomaterials are a center of interest owed to the large surface areas that is suitable for a variety of surface applications. The increase in demands for renewable energy generation significantly promoted rational design and assembly of a variety of 2D nanomaterials, the discovery of graphene since 2004. In 2D nanomaterials, charge carriers are confined along the surface while being allowed to move freely along the plane. Outstanding large planar area of 2D nanomaterials are highly sensitive to external stimuli, a characteristic property suitable for a variety of applications including electrochemistry. Because of their unique structures and multi-functionalities, 2D nanomaterials are inspiring great interest in energy conversion and storage field.

For this purpose, we have selected graphene and tungsten disulfide.

2.1 Graphene

Graphene is basically a carbon layer of one atomic thickness. It is also termed single-layer graphene (SLG). Graphene's desirable properties include its exceptionally high specific surface area, thermal conductivity, charge carrier mobility, transparency, and impermeability to gases. Graphene can be used to make two-dimensional (2D) nano sheets, which have drawn a lot of interest because of their uncommon characteristics and possible utilization in the fields of electronics, sensors, catalysis and energy.

It was discovered that electrons move ballistically in the 2D graphene structure with mobility greater than 15,000 $m^2 V^{-1} s^{-1}$. Graphene nanoribbons were hypothetically predicted and experimentally confirmed to show semi-conductivity if they had small widths and smooth edges. Graphene Nano sheets have high mechanical strength (>1060 GPa), high thermal conductivity (3000 $Wm^{-1} K^{-1}$), and high specific surface area (2600 $m^2 g^{-1}$). These very

specific properties make graphene a great additive to drastically improve the mechanical, thermal, and electrical properties of polymer materials. Alternative forms of the material are: few-layer graphene (FLG, »2–5 monolayers), multi-layer graphene (MLG, »2–10 monolayers), or multi-layered intricate structures.

The superior characteristics of graphene nanomaterials give them a remarkable technological significance. Graphene-based materials can be used in catalyst supports, membranes, and composites, and also in high-end applications such as energy generation and storage devices, gas sensors, printable electronics, and advanced electromagnetic properties.

2.2 Tungsten Disulfide WS_2

It seems natural to explore the graphene's analogues: as layered inorganic materials. Transition-metal dichalcogenides (TMDCs), e.g. MoS_2 , $MoSe_2$, WSe_2 and WS_2 , all of them consists of a hexagonal layer of metallic atom (M) e.g. W or Mo etc. which is sandwiched between two layers of chalcogen atoms (X) e.g S or Se etc. within the stoichiometric limit MX_2 . The collective feature of these materials is strong layered structure with covalent bonding within the each layer as well as weak Van der Waals forces between different MX_2 sheets. For these special characteristics, TMDCs have become the novel family offering great opportunities materials science. Single- and few-layered 2D nanosheets have been prepared successfully, via either mechanical or chemical exfoliation methods.[11]

WS_2, with the electronic properties complementary to that of semi-metallic graphene emerged as a new family of 2D materials. In such materials interest in potential applications in 2D semiconductors with remarkable electronic and optical properties has increased exponentially. WS_2 each layer consists of a slab S-W-S sandwiched layered structure by van der Waals. It possesses many characteristics properties in the monolayer regime, such as the indirect-to-direct bandgap transition, coupled spin and valley physics, and band structure with strain. Likewise, the combination of WS_2 with other 2D materials given rise to a large category of 2D heterostructures. **[12, 13]**

2.3 Synthesis Routes

The development of practical and reliable processes for the preparation of 2D nanomaterials to evaluate their properties, functionalities, and applications is very important. It is driven by

the fascinating properties and applications, great efforts are being devoted to the exploration of various synthetic routes to produce 2D nanomaterials. Many reliable synthetic routes are being developed, e.g. mechanical cleavage, ion-intercalation, liquid exfoliation, and selective etching and exfoliation, chemical vapor deposition (CVD), and wet-chemical synthesis. Generally, these methods are classified into two categories: top-down and bottom-up approaches. The top-down method based on the exfoliation of layered bulk crystals into single as well as few-layer nanosheets, in this various driving forces are used to break, weak Vander Waals interaction within the stacked layers. The bottom-up method is based on the direct synthesis of 2D nanomaterials from different originators, via chemical reaction. Two basic bottom-up routes are CVD and wet-chemical synthesis methods.[14]

Mechanical Cleavage

The mechanical cleavage method is an old route for the exfoliation of layered bulk crystals to obtain two dimensional flakes. In a general process, the bulk (e.g., graphite) is first attached onto a small piece of Scotch tape, and then another piece of Scotch tape is adhered onto the top of other crystal surface. After that, one piece of Scotch tape is detached from the crystal. This process can also be repeated many times to obtain flakes that are thin and can easily be transferred onto a target substrate (e.g., SiO_2/Si). Then, Scotch tape with the thin flakes is attached onto a target surface under normal pressure. In the end, the Scotch tape is peeled off from substrate and single or few-layer nanosheets (e.g., graphene) are easily found on the substrate**.[14]**

Ion-Intercalation and Exfoliation.

The ion-intercalation and exfoliation method relies on the intercalation of ions into the interlayer spacing of layered bulk crystals to weaken the van der Waals interaction between layers. The intercalated compounds obtained are then exfoliated into single or few-layer nano-sheets under sonication. The mostly common used intercalates are organometallic compounds, such as butyl lithium and metal naphtha-lenide (metal = Li, Na, K). In a typical process, when TMD crystals are simply immersed or refluxed in the intercalated solution (e.g., butyl- lithium), the cations can intercalate into the interlayer spacing of TMDs to form ion-intercalated compounds. Then, the well-dispersed single- or few-layer nanosheets can be easily obtained by sonication of the ion-intercalated compounds in water or ethanol. As a promising alternative, we developed an electrochemical method to intercalate Liþ ions into

layered compounds which allows us to monitor and control the amount of intercalated Liþ ions precisely and thus to achieve more efficient exfoliation.47□49 The layered bulk crystals coated on Cu foil and the Li foil are incorporated in a Li-ion battery cell as the cathode and anode, respectively (Figure 3a). Liþ ions are intercalated into the layered bulk crystals during the discharge process (Figure 3a). This ion-intercalation and exfoliation method has successfully been used to prepare many ultrathin 2D nanosheets from their layered bulk crystals, such as graphene, h-BN, and many TMDs (e.g., MoS2, WS2, TiS2, TaS2, ZrS2, NbSe2, WSe2, Sb2Se3, and Bi2Te3) significantly, the production yields of this method are high. Among them, the yields of single-layer MoS2 and TaS2 sheets are over 90%. This method has a unique advantage as well: the Li-intercalation in TMD crystals can induce the phase transformation of TMD from the semiconducting 2H phase to the metallic 1T phase dur- ing the exfoliation process. Phase engineering of ultrathin 2D TMDs gives rise to great opportunities for realizing superior performance**.[14]**

Chemical Vapor Deposition.

The CVD method is another typical bottom-up process used to prepare ultrathin 2D nanomaterials on substrates. In a typical process, the given substrate is exposed to reactive precursors at high temperature and high vacuum, in which the precursors react and/or decompose on the surface of the substrate to form ultrathin 2D flakes or large-area ultrathin films. It is worth emphasizing that this method allows us to produce ultrathin 2D nanomaterials with high crystal quality, scalable size, tunable thickness, and excellent electronic properties. To date, this method has been successfully utilized to prepare many ultra- thin 2D nanomaterials including graphene, TMDs (MoS2, WS2, MoSe2, WSe2, ReS2, GaS2, etc.), h-BN, topological insulators (e.g., In2Se3 and Bi2Se3), and metal oxides. Promisingly, the growth of large-area uniform graphene in wafer scale or even square meters has been achieved, holding great promise for many practical applications. How- ever, high temperature and high vacuum are normally used in the CVD growth process. In addition, a specific substrate is necessary to support the grown ultrathin 2D nanomaterials, resulting in the requirement of a transfer process to move the obtained 2D nanomaterials onto desired substrates for further studies and applications. Remaining challenges for this method include: (1) how to achieve the growth of ultrathin 2D nanomaterials on arbitrary substrates in order

to avoid the complicated transfer process that is currently used and (2) how to grow high-quality ultrathin 2D nanomaterials at low temperature, which would make the CVD method simple and more efficient**.[14]**

Wet-Chemical Synthesis.

Wet-chemical synthesis is another typical bottom-up method that has been widely used to produce ultrathin 2D nanomaterials. Wet-chemical methods are used to synthesize target materials from certain precursors via chemical reactions in solution, in which surfactants are normally used to control the size, shape, and morphology as well as to stabilize the synthesized materials. Some widely used wet-chemical methods for nanomaterials include templated synthesis, hydro/solvo thermal synthesis, self-assembly of nanocrystals, and soft colloidal synthesis. Wet-chemical methods have been demonstrated to be effective for synthesis of numerous ultrathin 2D nanomaterials, such as graphene-BN, g-C3N4, TMDs (e.g., MoS2, TiS2, TaS2,WS2, and ZrS2), metals, metal oxides, metal chalcogenides, LDHs, MOFs, COFs, and polymers. It is worth pointing out that almost all the nonlayer structured ultrathin 2D nanomaterials, such as metals (e.g., Au, Pd, and Rh), metal oxides (e.g., TiO2, CeO2, In2O3, SnO2, and Fe2O3), and metal chalcogenides (e.g., PbS, CuS, SnSe, ZnSe, ZnS, and CdSe), can be synthesized by wet-chemical synthesis methods.143 Importantly, the wet-chemical synthesis enables the realization of high-yield and massive production of ultrathin 2D nano-materials in liquid at relatively low cost, which is potentially applicable for industrial production. In addition, size and shape control of ultrathin 2Dnanomaterials is easier to achieve in wet-chemical syntheses in comparison with other methods. However, it is hard to obtain single-layer nanosheets for most of the nanomaterials synthesized by wet-chemical methods, because the synthesis is easily affected by reaction parameters, including reaction temperature, reaction time, concentration of precursors, and solvents**.[14]**

Liquid Exfoliation

Liquid exfoliation is another best process that is extensively used to exfoliate layered bulk crystals to get ultrathin 2D nanosheets. It is used to exfoliate layered bulk crystals directly in solvents, e.g. N-methyl-pyrrolidone (NMP) and dimethylformamide (DMF), via bath/probe sonication. In this process, the sonication process breaks the weak van der Waals interaction between different layers, but cannot destroy the covalent bonding. It is found that good

matching of the surface tension of the layer crystal and solvent is the key factor in controlling the energy and increasing the efficiency of exfoliation. Furthermore, the solvent is as important in balancing the exfoliated nanosheets and barring their restacking and aggregating. Moreover, the solvents used in exfoliation should be organics.

Many 2D nanomaterials, graphene, h-BN, TMDs, metal oxides, metal hydroxides, MOFs, BP, are being prepared by this method from the layered bulk crystals. It is important that this method enables the high-yield and mass production of 2D nano-materials in solution at very low cost, because the process is so simple**.[14]**

2.4 Motivation and Objectives

Two dimensional (2D) nanomaterials are very attractive due to their unique structural and surface features for energy storage applications. Motivated by the recent pioneering works demonstrating the emergence of 2D nanomaterials, the energy storage and nanoscience communities can revisit bulk layered materials though state-of-the-art nanotechnology. However, no review has focused on the fundamentals, recent progress, and outlook on this new mechanism of 2D nanomaterials yet. In this study, the key aspects of emergent GO/WS_2 LBL heterogeneous based structure on 2D nanomaterials will be comprehensively reviewed, which will be covering the history and classification, electrochemical characteristics, and design guidelines, thermodynamic and kinetic aspects of materials for extrinsically surface reactions. The structural and compositional controls of both graphene and tungsten disulfide on both microscopic and macroscopic levels will particularly be addressed, emphasizing will be on the importance of valuable results. Finally, our perspectives on current impediments and future directions of 2D nanomaterials on this field will be offered. Infinite combinations and modifications of 2D nanomaterials could a rational strategy to overcome intrinsic boundaries of available materials, offers a next-generation energy storage materials toward a high end and new position in the field.[15]

Two-dimensional (2D) nanomaterials become a versatile platform for the creation of innovative hybrid materials with various functionalities due to their uniqueness in electrical, optical, thermal, and mechanical properties. The preparation of graphene-based composites with precision is very important for reproducibility as well as controlled performance through the analysis of chemistry between each component. Specially, the layer-by-layer (LbL)

assembling technique is known as a simple, inexpensive, and fast process for the production of highly ordered multilayer films structure in various types of materials. The LbL structures are capable of controlling the nanoscale composition and architectures can be achieved through the sequential adsorption of differently charged components by the attractive forces e.g. electrostatic interactions. Multilayered graphene, composites exhibit improved physical/chemical properties as well as superior performance compared to the individual components due to the synergistic effects in multiple applications e.g. electric devices, and biological usages, energy storage and conversion.[16]

Multilayer: Graphene and WS_2 nanosheets were fabricated and assembled through layer-by-layer (LBL) assembly. By using a filtration system on a polymer to enhance the electrochemical performance of the films that were investigated to evaluate their potential as electrode materials to be used in supercapacitor devices. The WS_2 /GO multilayer films exhibited a high specific capacitance of 880 F/g and area capacitance of 70 F/m^2 under the scan rate of 5 mV/s. And the film exhibited good cycle stability over 2000 cycles. A flexible electrode can be deposited onto PET substrate to show the potential of Multilayer heterostructured films for flexible energy storage.[17]

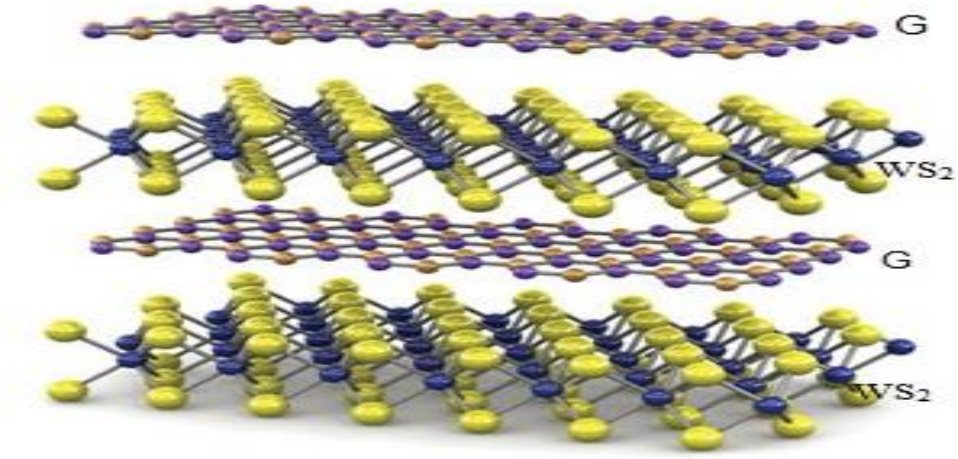

Fig: Layer By Layer Assembly design for super capacitors.

Chapter 3: Synthesis Process and Methodology

The high-volume synthesis of two-dimensional (2D) materials in the form of platelets is desirable for various applications. Here we exfoliate 2D materials by chemical exfoliation which is the best process extensively used to exfoliating layered bulk crystals to get ultrathin 2D nanosheets. It is used to exfoliate layered bulk crystals directly in solvents, e.g. N-methyl-pyrrolidone (NMP) and dimethylformamide (DMF), via bath/probe sonication. In this process, the sonication process breaks the weak van der Waals interaction between different layers, but cannot destroy the covalent bonding. It is found that good matching of the surface tension of the layer crystal and solvent is the key factor in controlling the energy and increasing the efficiency of exfoliation. Furthermore, the solvent is as important in balancing the exfoliated nanosheets and barring their restacking and aggregating. Moreover, the solvents used in exfoliation should be organics. Many 2D nanomaterials, graphene, h-BN, TMDs, metal oxides, metal hydroxides, MOFs, BP, are being prepared by this method from the layered bulk crystals. It is important that this method enables the high-yield and mass production of 2D nano-materials in solution at very low cost, because the fabrication by this method is very simple and fast

3.1 Liquid Exfoliation

Apart from mechanical techniques, numerous recent procedures for exfoliation are reliant upon the ultrasonication of a liquid suspension (dispersion) containing the sample crystals in bulk. This causes energetic agitation. The ultrasonic waves spread throughout the solvent, resulting in cycles of low and high pressure (in an alternating manner). These cycles help in the process. Two distinct types of forces are generated by the cycles: vibration and cavitation. The procedure of liquid exfoliation depends upon the uninterrupted subjection of the crystals to the vibration and cavitation energy inputs, so that they can be thinned constantly, up

until two-dimensional nanosheets can be extracted from the solvent by centrifuging it.

It is believed that exfoliation using a liquid as a solvent (dispersion media) is a feasible method of producing nanosheets on a large scale. It is easy to achieve thin films from such a suspension and make hybrids and nanocomposites to find out more about nanosheets. This has caused a considerable increase in interest in this approach. Using a Probe or Bath Sonicator is the most widely-used method to get two-dimensional nanosheets by shear forces acting on the sample.[18]

When, in conventional approaches, we transmit ultrasonic waves into the solvent using a probe or even an ultrasonic horn, cavitation modes are generated in the solvent, in addition to the vibrational modes. In the lamellar crystals, the vibrational modes are generated due to the propagation of the ultrasonic wave throughout the solvent. When the power is sufficient, the vibrational modes overcome the van der Waals forces in the Graphene/WS_2 flakes, as the action of the compressional wave on the material surface combines with a tensile stress wave reflected back on the material body, getting two-dimensional nanosheets from the bulk. As we increase ultrasonic power, we can generate cavitation forces having higher energy. Apart from aiding the exfoliation process, these modes also result in nanosheet breakage. Vibrational modes results in some minor chipping, which is basically breakages occurring at the nanosheets' outer surfaces. This causes a reduction in the lateral dimensions of the nanosheets. Vibrational modes are not as efficient, but allow us to preserve the sheets' dimensions. There has to be a compromise between vibrational and cavitation modes, contingent upon the desired properties of the material we want to achieve.

3.2 Factors to consider for exfoliation

i) Solvent selection

For efficient exfoliation, we must carefully select the solvent to be used. The solvent has three parts to play in the process:

(1) Medium (for effective transfer of the ultrasonic energy from the sonicator to the sample)

(2) Solvent with the desired requirements (to keep the enthalpy of mixing at a minimum)

(3) Steric barrier inhibiting agglomeration and re-stacking of the nanosheets, thus making them more stable.

Variables such as relative permittivity and surface tension are used to assess the efficiency of solvents. Solvents from the N-alkylpyrrolidone family, e.g. N-methyl-2-pyrrolidone (NMP) and N-cyclohexylpyrrolidone (CHP) are especially effective, seeing as we can achieve highly concentrated nanosheet dispersions that have long-term stability. [18]

ii) Sonication power and type

Two kinds of ultrasonic probes are accessible to us: the bath sonicator and the probe sonicator. By researching their effectiveness in exfoliating graphene, it was found that the probe tip has a larger output of energy and we can apply this energy in a more direct manner. This being said, these graphene nanosheets were found to be smaller in their lateral dimensions as compared to those we got from bath sonication. The higher power is probably the causative factor for the nanosheet breakage. We can select the input according to the kind of nanosheets we desire to achieve.[18]

The optimum power is in between 250 and 320 W; at lower power, inhibition of cavitation occurs, giving us lesser energy for exfoliation, while, on the other hand, at over 320 W, cavitation is suppressed by the large number of cavitation bubbles in the solvent. Lesser power decreases the concentration of material which has been exfoliated, but increases the dimensions (lateral dimensions as well as thickness) of the sheets.[18]

iii) Sonication time

We have to be careful while increasing time of sonication as this causes nanosheet breakage, thus lowering the lateral dimensions in addition to reducing thickness. Optimum relationships between size and number of nanosheets are usually

achieved in sonication times of 48 to 60 hours. This gives us sheets in the size range of 500 to 800 nm. [18]

iv) The use of additives

Increased research in the area of exfoliation has led us to use mixtures of solvents and surfactants on a large scale. These approaches also have the advantages of low costs and reduced effect on the environment.

The surfactant has two purposes:

(1) Regulates the solvent's surface tension to increase the dispersibility.

(2) Becomes adsorbed onto the nanosheet surfaces, thus causing a repulsion force, hindering agglomeration. [18]

If the surfactant can match both the surface tensions at the solid-liquid interface, the particular kind of surfactant we select is not too important. By correctly selecting surfactants, we can produce numerous dispersions of Graphene/transition metal dichalcogenides in more suitable solvents. The concentrations of the dispersion and surfactant are correlated; as exfoliation is being done, surfactant adsorption results in increasing surface tension, thus hindering further exfoliation. We can maintain the surface tension better by adding a constant amount of surfactant. This allows unhindered exfoliation and higher yield.[18]

v) A size selection process

Normally, optimum liquid exfoliation (done with a probe sonicator, with between 48 and 60 hours' sonication time, using N-methyl-2-pyrrolidone as solvent) gives us a tungsten disulfide dispersion of ≈ 10 mg/mL; having an average thickness of 3 to 4 layers. That being said, such dispersions have nanosheets with a wide distribution of lateral dimensions (50 nanometers – 2 microns in the same sample). We can select and extract the desired size of nanosheets by centrifugation. In

addition, we can perform sediment recycling to get nanosheets with smaller dimensional ranges.[18]

vi) The source of precursor

Mostly, the precursor is the powdered material available in the market. Experiments carried out with MoS_2 found that sonicating the pure powder and the mineral MoS_2 gave us similar nanosheets which were highly crystalline and had lateral dimensions between 200 nanometers and 1 micron. This may have a significant adverse effect on the electronic characteristics of the nanosheets produced but allows us to fabricate the same material for other surface active applications using a less costly method.[18]

vii) Liquid-mediated exfoliation: further developments

Scientists are trying to increase nanosheet production scalability, since liquid exfoliation has been highly developed by now. High-shear mixing as well as jet cavitation have been found to be feasible options instead of conventional exfoliation approaches. Specifically, high-shear mixing has been found to have an effective application in the form of tungsten disulfide exfoliation. Instead of depending upon vibrational and cavitation energy to aid exfoliation, a group of researchers has utilized shear forces in a direct manner by making use of a high-shear mixer and a household blender, to achieve two-dimensional nanosheet dispersions more efficiently. This significantly affects the procedure, because of its cheapness, easier scalability and its capability to make transition metal dichalcogenides dispersions of high concentrations. Taking this into consideration, researchers have systematically investigated the optimum conditions for nanosheet exfoliation, while considering several parameters.

3.3 Methodology

Sample	**Graphene**	**WS_2**
Type (Powder)	(0.5µm)	(0.5µm)
Dispersive Media (60ml)	N-Methyl-2-Pyrolidone	N-Methyl-2-Pyrolidone
Weight (g)	1.2g	1.2g
Concentration	20mg/mL	20mg/mL
Sonication Temperature	25 ºC	25ºC
Sonication Time (hours)	48h	48h
Centrifuged* (rpm)	1500, 1000, 500 rpms	1500, 1000, 500 rpms

Table: Methodology adopted

*2D nanosheets centrifuged at 1500,100,500 rpm were separated into different veils.

Centrifuge samples were vacuum filtered on 0.5 micron pore size filter paper to separate nanosheets from the liquid (NMP). After filtration filter paper were placed in a furnace to dry for 5hrs at 80ºC. Each filter paper was weighed on analytical weight balance to know the yield of nanosheets obtained at different rpms (1500, 1000, 500rpm).

Graphene 500	0.0831g
Graphene 1000	0.1233g
Graphene 1500	0.0954g
Tungsten disulfide WS_2 500	0.1108g
Tungsten disulfide WS_2 1000	0.0833g
Tungsten disulfide WS_2 1500	0.0157g

Table: Nanosheets yield by weight.

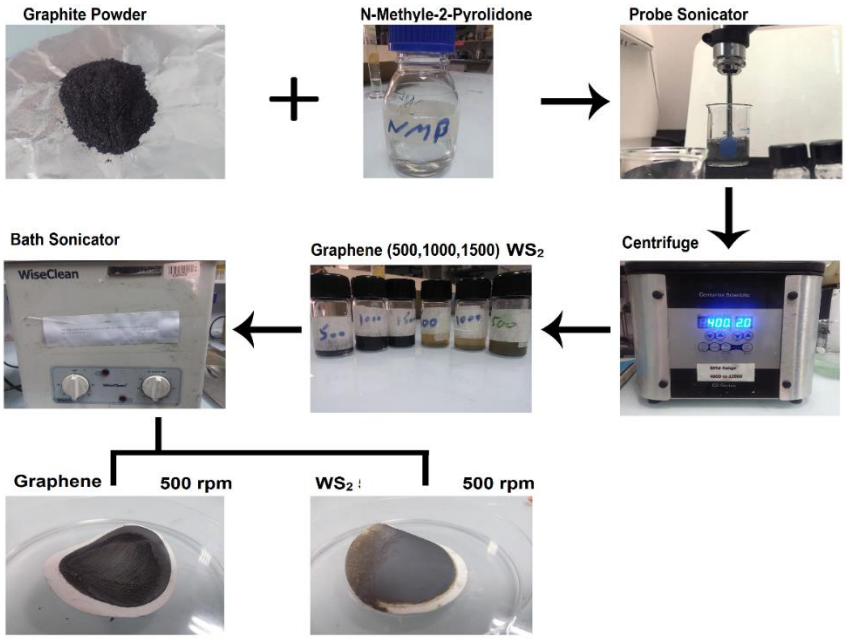

Fig: Procedure Flowchart

Methodology is optimized to improve the quality, reduce the time and cost.

Chapter 4: Characterization Techniques

4.1 Structural Characterization

- **X-Ray Diffraction (XRD Analysis)**

  Powder X-Ray Diffraction gives comprehensive information on the crystallographic structure and physical properties of materials and thin films.

  In this process, a monochromatic X-Ray beam is incident on the sample, the angle range for which is adjusted according to our requirements. The X-Rays interact with sample atoms, causing diffraction (provided that the Bragg equation is fulfilled). Characteristic spectra of chemical phases and composition are obtained. A feature unique to this method is the ability to identify phases. Added to this, we can also quantify phases, find out the crystallinity by percentage, the size of the crystallites, and the size of the unit cell.

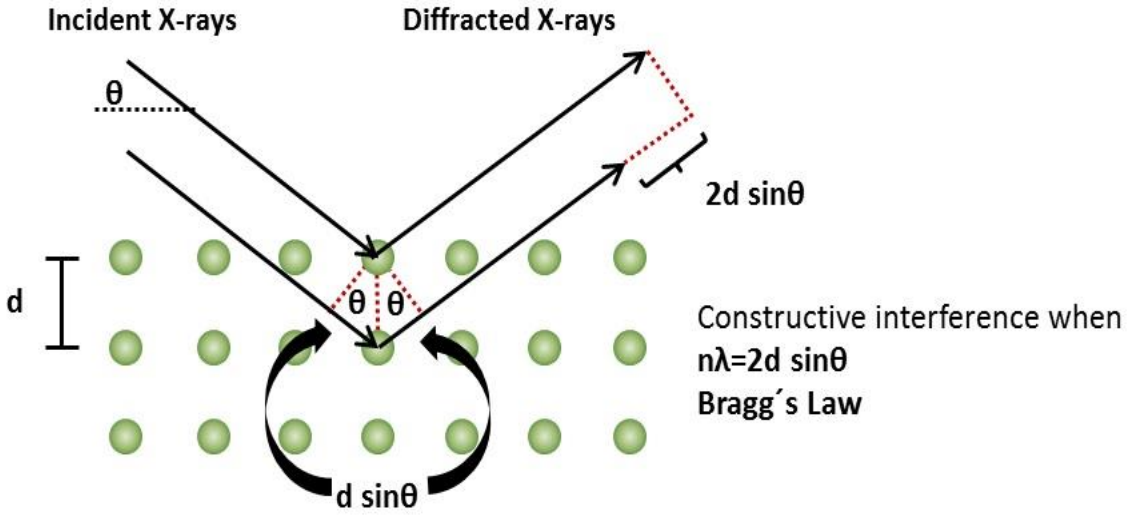

4.2 Optical Characterization

- ***Scanning Electron Microscope (SEM)***

  In SEM, a fine probe of electron beam is focused and scans over the specimen's surface. Interactions of these electrons with the surface results in the electron or photon emission and a substantial portion of these emitted electrons/photons are collected by the detector. The output from detector modulates the brightness of cathode ray tube (CRT). For every point the electron beam strikes on the specimen's surface is plotted onto a corresponding point on the CRT and an image is produced.

  The electron-surface interactions cause generation of secondary electrons (SE), backscattered electrons (BSE), and X-rays. SEs are low energy electrons emitted from resulting from inelastic scattering of primary electron beams scanning over the surface of specimen. BSEs are the high energy elastically scattered electrons of primary electron beam which are reflected out of the specimen's surface. X-rays can also be generated when high accelerating electrons impinge upon the specimen's surface. Using appropriate detector types, information about surface topography, phase contrast and chemical composition (in elemental form) can be generated.

  The SEM provides a magnified image of specimen's surface. Magnification of SEM can be as high as 300,000X with resolution approaching a few nanometers. SEM not only provides with surface topographical information but the composition of regions near the surface of material as well[66].

  SEM analysis was performed using scanning electron microscope (JEOL-JSM-6490LA) with operating voltage of 10-20 kV, spot size of 35-60, and working

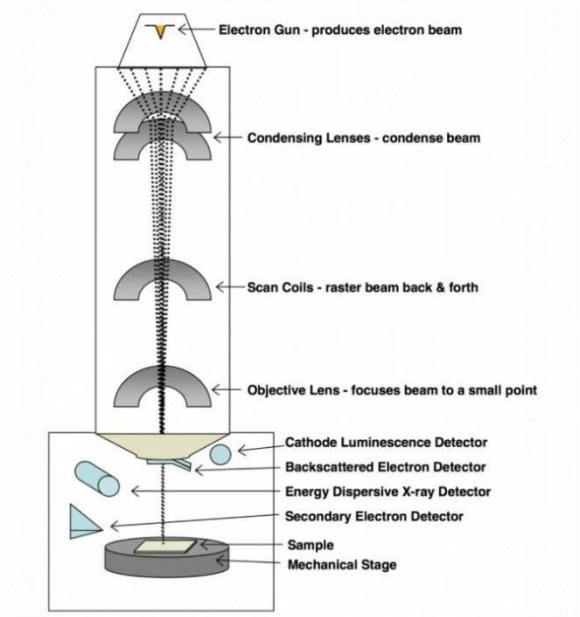

distance of 10mm. The images were recorded in SE mode at low and high magnifications. Two-dimensional (2D) nanomaterials become a versatile platform for the creation of innovative hybrid materials with various functionalities due to their uniqueness in electrical, optical, thermal, and mechanical properties. The preparation of graphene-based composites with precision is very important for reproducibility as well as controlled performance through the analysis of chemistry between each component. Specially, the layer-by-layer (LbL) assembling technique is known as a simple, inexpensive, and fast process for the production of highly ordered multilayer films structure in various types of materials. The LbL structures are capable of controlling the nanoscale composition and architectures can be achieved through the sequential adsorption of differently charged components by the attractive forces e.g. electrostatic interactions. Multilayered graphene, composites exhibit improved physical/chemical properties as well as superior performance compared to the individual components due to the synergistic effects in multiple applications e.g. electric devices, and biological usages, energy storage and conversion.[16]

Multilayer: Graphene and WS_2 nanosheets were fabricated and assembled through layer-by-layer (LBL) assembly. By using a filtration system on a polymer to enhance the electrochemical performance of the films that were investigated to evaluate their potential as electrode materials to be used in supercapacitor devices.

The WS_2 /GO multilayer films exhibited a high specific capacitance of 880 F/g and area capacitance of 70 F/m^2 under the scan rate of 5 mV/s. And the film exhibited good cycle stability over 2000 cycles. A flexible electrode can be deposited onto PET substrate to show the potential of Multilayer heterostructured films for flexible energy storage.[17]

Fig. shows the JSM-6490LA SEM present in School of Chemical and Materials Engineering, National University of Science and Technology, Islamabad.

Fig. shows schematic of a typical SEM.

Fig. JOEL JSM-6490LA present at SCME; (b) SEM Schematic

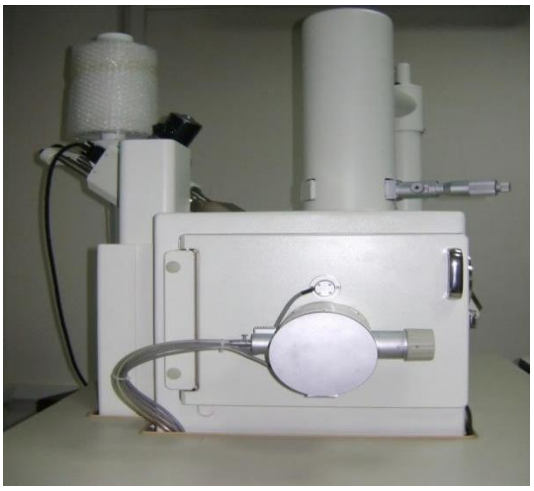

- ***Atomic Force Microscope (AFM)***

AFM use a pointed tip on a flexible cantilever. A tip scans over the sample, whenever the tip comes within a few angstroms of the surface of specimen repulsive van der Waals forces is generated between the atoms on the tip and those on the sample's surface which cause the cantilever to deflect. AFM employs a piezoelectric scanner to scan the tip across the sample and a feedback control operates on the scanner to maintain a constant separation between the tip of AFM and the sample's surface. An optical-lever is used for monitoring the deflection in which light bean from a laser diode is reflected from the cantilevers' back on a position-sensitive photodiode. Position-sensitive photodiode is extremely sensitive thus the vertical resolution of AFM is sub-Å whereas the lateral resolution of AFM is about l nm. Figure 3-4 (a) and (b) show images of SPM available in SCME.

JEOL JSPM 5200 was used in tapping mode on an area of 2×2 μm^2 for measuring of roughness of surface and imaging the topography of deposited films. The AFM studies were performed in air through operation in a tapping mode to maximize the

tip–sample interactions. The probes used were micro-fabricated cantilevers (NSC35; μmasch) with respective values of length, nominal tip radius, spring constant, and resonance frequency to be 130 mm, 10 nm, 4.5 N/m, and 150 kHz.

Fig.: (a-b) Scanning Probe Microscope at SCME, NUST

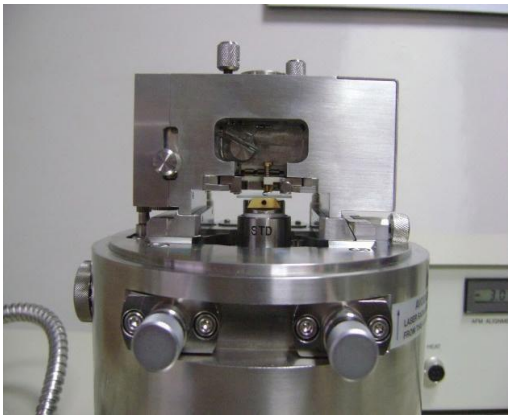

4.3 Optical Characterization

- **UV-Vis Spectrophotometer**

Optical properties such as percent transmission, absorption, and reflectance can be determined using a spectrophotometer. A spectrophotometer involves collimated electromagnetic (EM) radiations from ultraviolet (UV) to the far

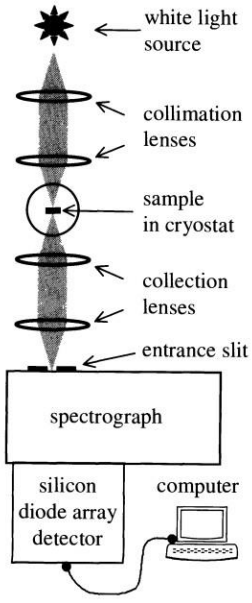

Fig.: (a) Schematic diagram of an experimental arrangement to measure absorption spectra in the wavelength range 200-1000 nm using a silicon diode array detector (b) UV-Vis spectrophotometer meter in SCME, NUST
Absorption and % Transmission data was recorded using Jenway 7315 UV-Vis spectrometer in wavelength range of 200-900 nm of electromagnetic spectrum.

infrared region (IR) range of the electromagnetic spectrum that are incident onto the specimen. The intensity of the transmitted beam is calculated over range of the wavelength of incident radiations. Parameters are wavelength (λ) of incident beam, its energy (hν), and the wavenumber (WN). The most common unit for wavelength is nanometer. A spectrophotometer measures intensity as a function of λ of the light source.

Chapter 5: Results and Discussions

5.1X-Ray Diffraction (XRD)

- **Graphene**

X-ray diffraction was performed in order to judge the efficiency of transforming graphite into graphene.

The diffraction patterns for graphite indicates a highly intense peak, at 2θ = 26.65°, telling us that the basal spacing is 0.334 nm, prior to a peak at 54.92°, both of which are characteristic of graphite.

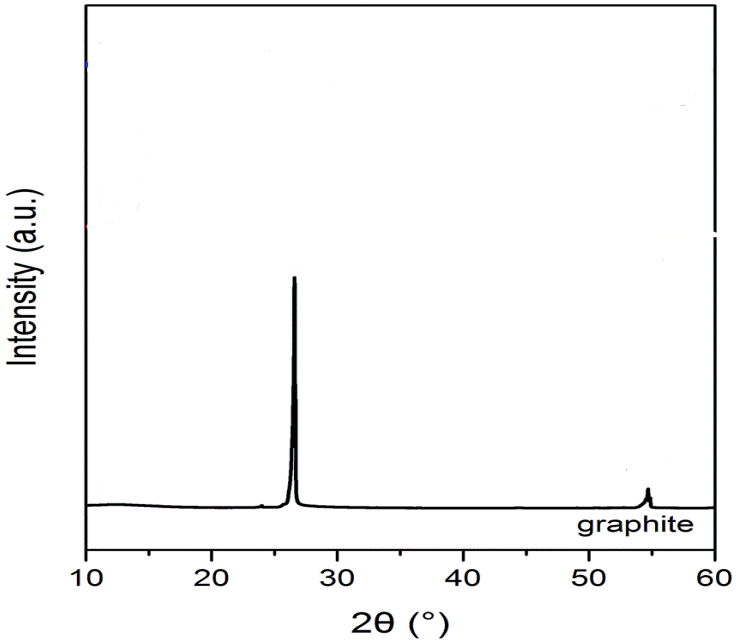

Fig. XRD diffraction pattern of graphite.

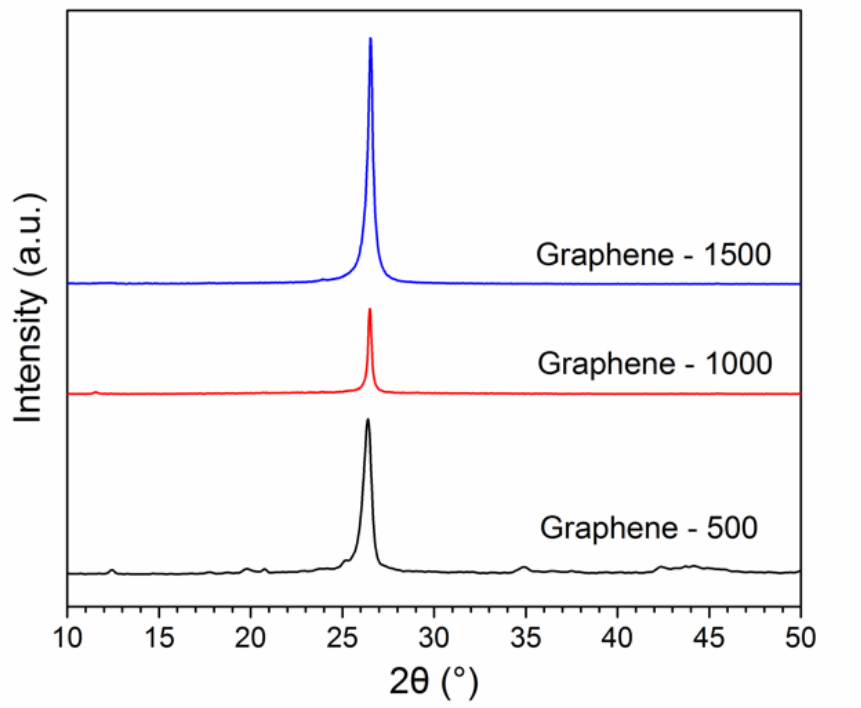

Fig. XRD diffraction patterns of exfoliated graphene 1500 at top, graphene 1000 in the mid, graphene 500 at bottom.

The diffraction pattern of graphene indicates a highly intense peak at 26.5°, indicating the formation of graphene nanosheets with the same basal spacing as natural graphite.

- **WS_2**

In the diffraction pattern of tungsten disulfide nanosheets, the peaks indicate well-resolved crystallized tungsten disulfide nanosheets achieved through exfoliation. A weak peak is indexed to the (002) plane, at 2Θ=14.50, which is evidently lower than that of commercial tungsten disulfide powder. In our belief, the intensity of the peak has been influenced by the sample preparation which has caused restacking of the nanosheets. The diffraction pattern obtained proves the same. The intensity of the (002) plane of WS_2 sheets, is weaker than that of bare WS_2 sheets, indicating the intercalation of WS_2 sheets. The other diffraction peaks can be attributed to the filter paper on which WS_2 was placed.

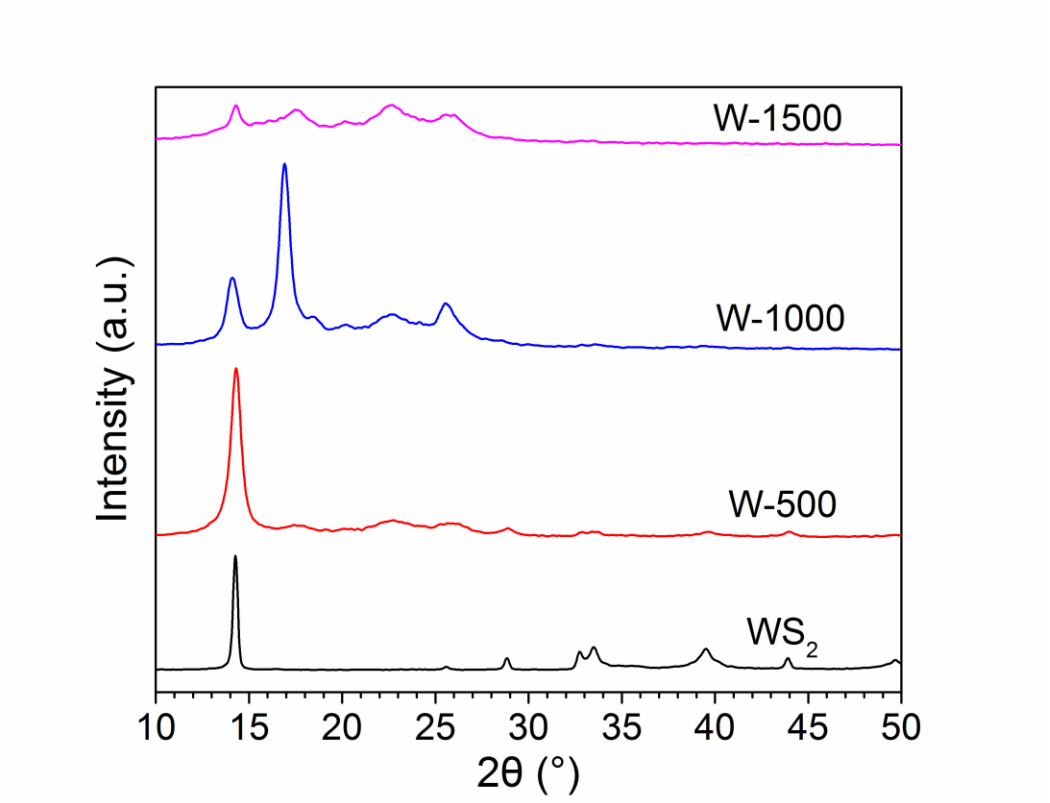

Graph: XRD graph for Tungsten Disulfide, WS_2.

The shift in peaks indicates the structural variations in the process of exfoliation when compared to WS_2 powdered form. Sheets exfoliated and separated at different rpm also show structural change due to different lateral size nanosheets.

Extra peaks rather than characteristic peaks of WS_2 are due to the filter paper on which sample was stick in the form of 2D sheets.

5.2Scanning Electron Microscopy (SEM)

- **Graphene**

The morphology and microstructure of the as-prepared samples were investigated by SEM the typical SEM images of the obtained samples at different magnifications are shown in Fig. The low-magnification SEM image, the prepared WS2 samples were mainly made up of a large number of nanosheets.

To further expose the microstructure of these sheets, the high-magnification SEM image is also observed. It shows that the prepared nanosheets are nearly monodisperse and stacked loosely, and the width of the nanosheets is in the range of 3.81–4.22 μm for graphene nanosheets centrifuged at 500 rpm.

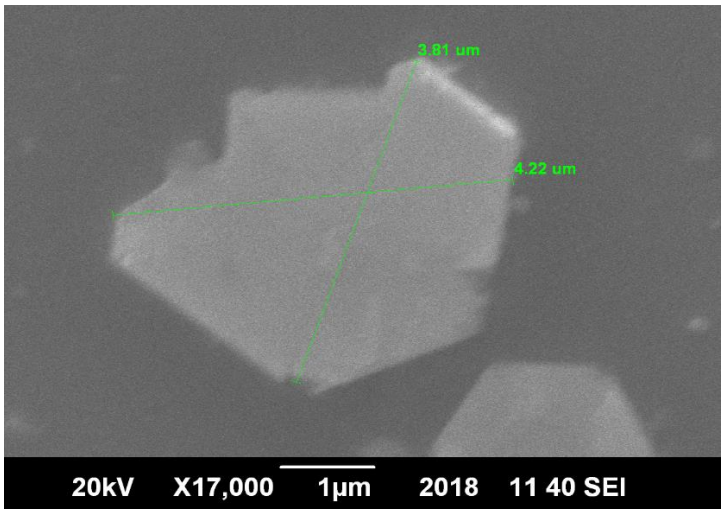

The result that we obtained from SEM for Graphene at 500 rpm.

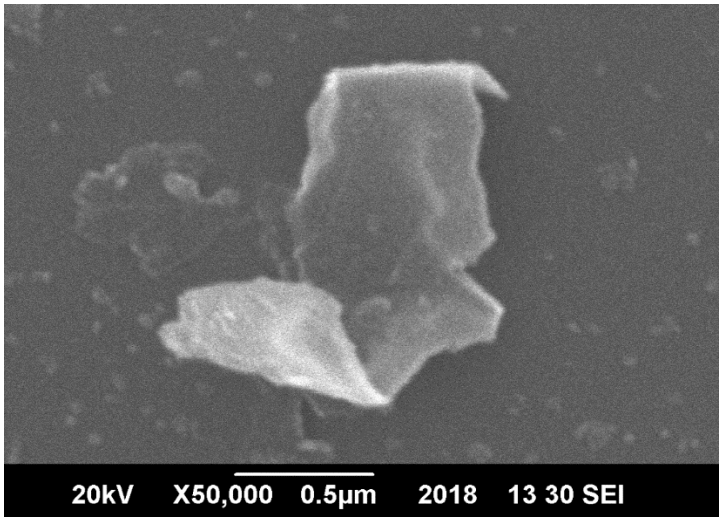

The result we obtained for Graphene at 1000 rpm, from SEM

The lateral dimensions for nanosheets decreased by increasing the centrifuge speed. Much higher lateral dimension nano sheets are obtained for graphene 500 rpm sample 3.81-4.22 μm and smaller sizes are obtained for 1500 rpm in the range of 348-653 nm.

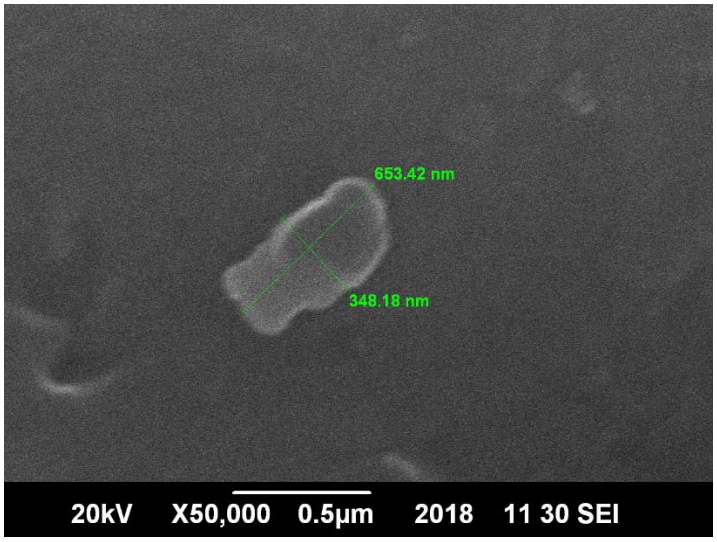

The result that we obtained from SEM for Graphene at 1500 rpm

- **WS_2**

  It can be noted that a fraction of WS_2 nanosheets were slightly curved. The reason may be that such ultrathin 2D materials are unstable and easily form closed structures by rolling up in order to eliminate dangling bonds at the edges. The width of the nanosheets is in the range of 1.79-2.10 µm for WS_2 nanosheets centrifuged at 500 rpm.

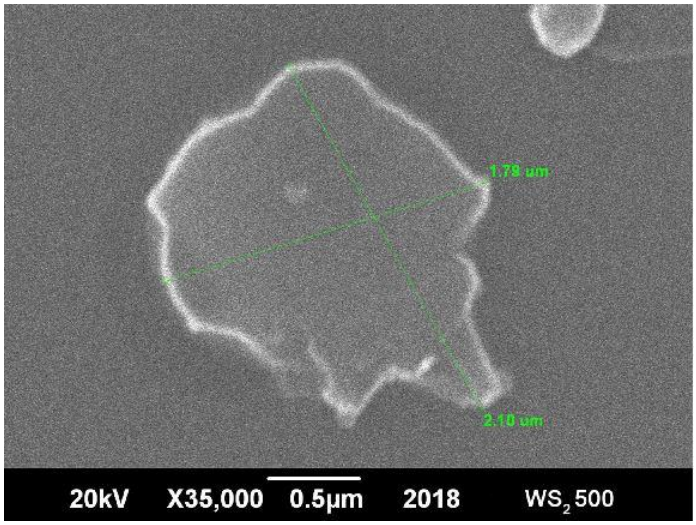

The result that we obtained from SEM for WS_2 at 500 rpm

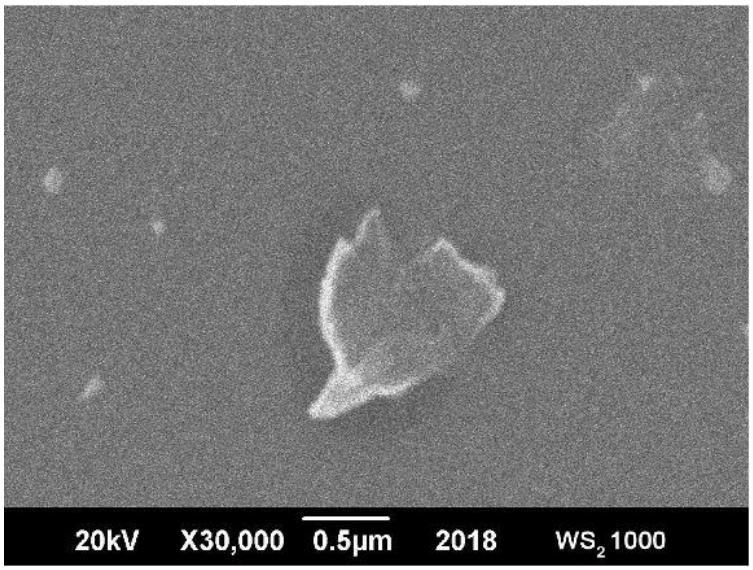

The result that we obtained from SEM for WS_2 at 1000 rpm

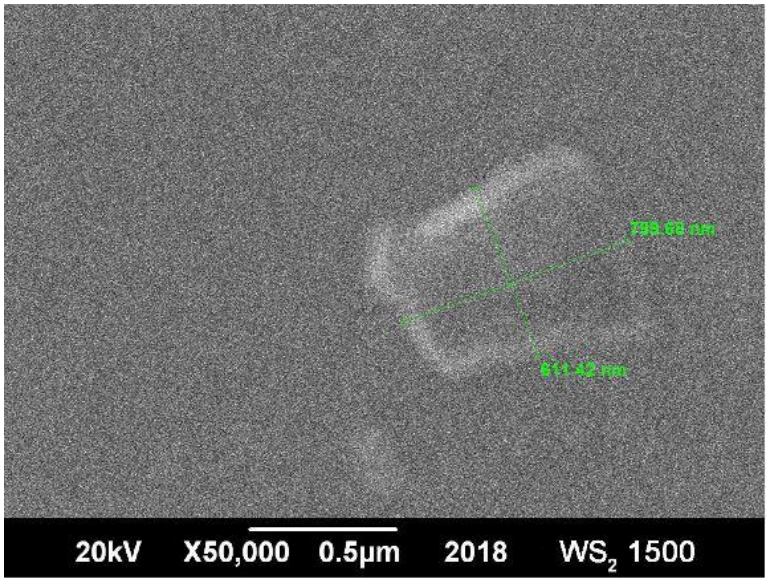

The result that we obtained from SEM for WS_2 at 1500 rpm

The width of the nanosheets is in the range of 799-611 nm for WS_2 nanosheets centrifuged at 1500 rpm.

5.3Atomic Force Microscopy (AFM)

AFM has so far been the main method for directly identifying and confirming the thickness and roughness of single- and few-layer graphene. It played a vital role in the discovery of graphene. The definitive evidence that the thin flakes in the supernatant obtained by our method are only a single layer thick or a few layers is obtained with the AFM.

➢ Graphene

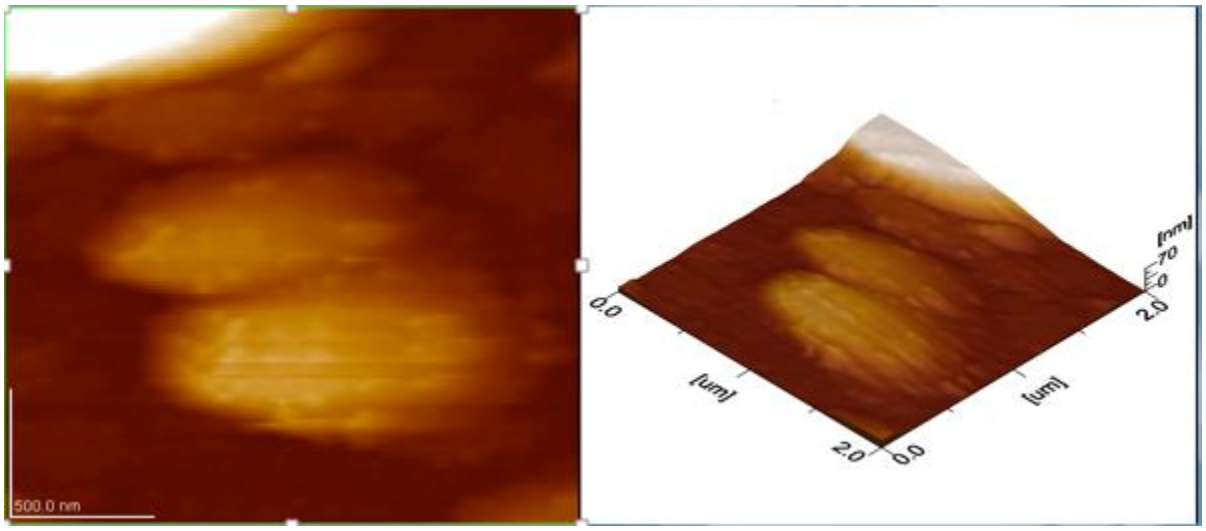

Fig. shows the typical results of AFM for graphene nanosheets.

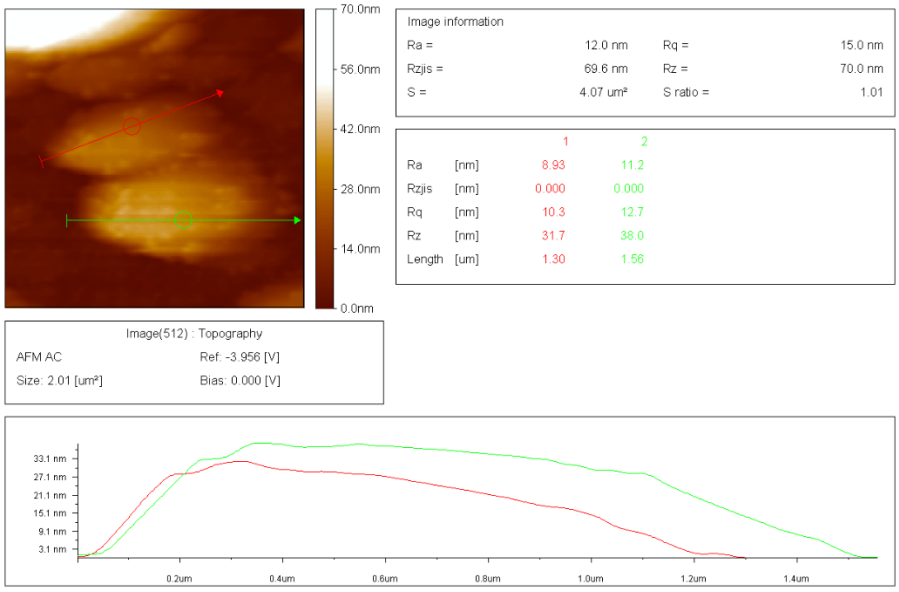

So the graphene sheets with the measured length of 12.7nm and width of 11.2nm shows the lateral dimensions. The topographic image in can be identified as multilayer with a measured thickness stacked layers of 69.6 nm. It shows the situation of a monolayer stacked on each other. Hence this statistically proves the above results all over the AFM image. Therefore, the AFM results firmly shows the presence of multilayer stacking of 2D nanosheets for graphene.

- **WS_2**

The monolayer nature of the exfoliated sheets of WS_2 was confirmed by atomic force microscopy (AFM). Based on the AFM analysis of the exfoliated sheets have a dominant lateral size of about 6.67 nm. Normally, individual sheets measured by AFM have an average thickness of∼1.2 nm, in line with the reported apparent thickness of a chemically exfoliated monolayer of WS_2. Note that this value is somewhat larger than the theoretical thickness of monolayer WS_2.

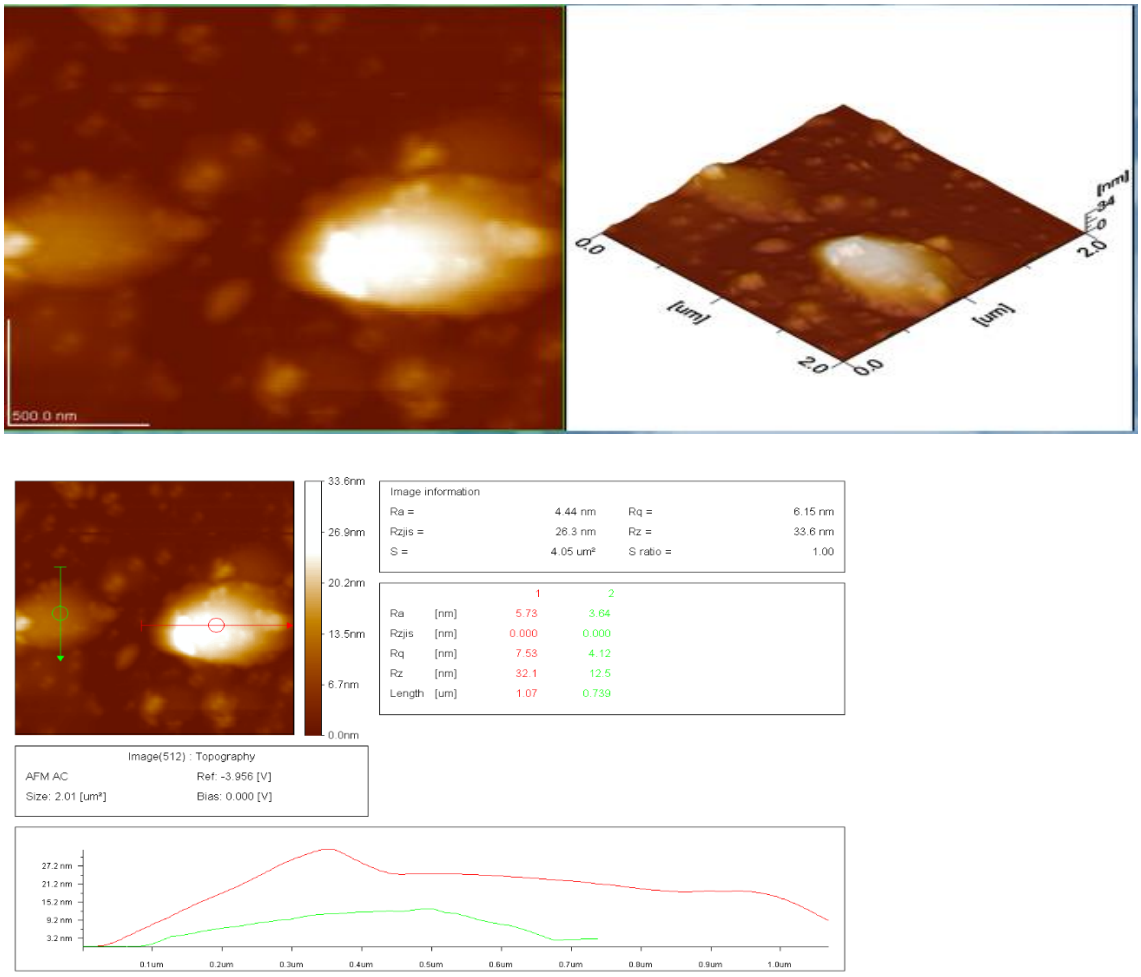

Fig. shows the typical results of AFM for WS_2 nanosheets.

5.4UV-Vis Spectroscopy

- **Graphene**

The initial monitoring of the formation of nanosheets was carried out by measuring the UV–Vis spectra of graphene. The Graphene has absorption band ~301 nm, whereas, a characteristic switch from ultra violet to visible band at ~539 nm was observed. No absorption band was observed for graphene in the range above 301 nm. Which is the characteristic of graphene.

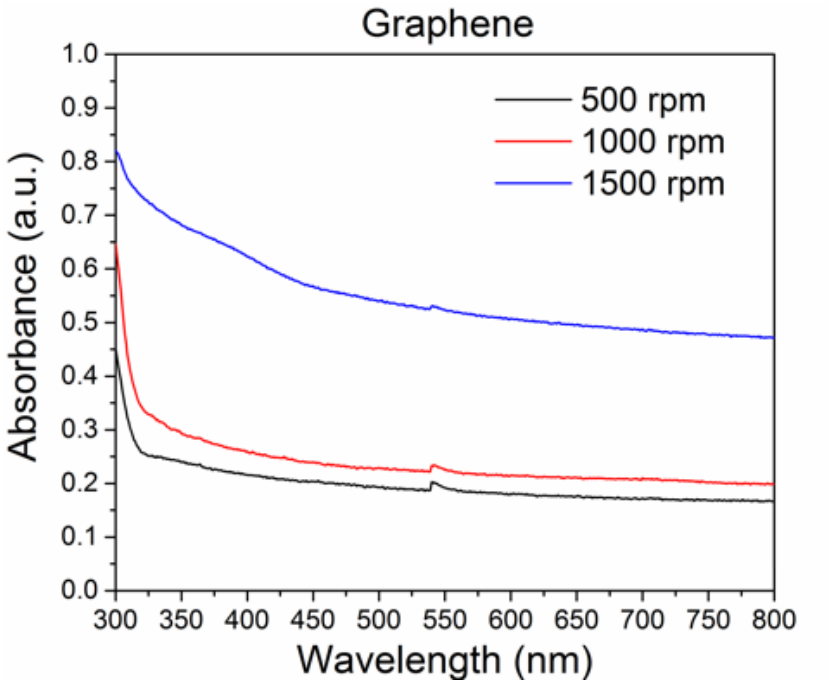

The results that we obtained through UV-Vis Spectrometry for Graphene.

The bottom line graph shows the curve of absorbance against wavelength values in nanometers, for Graphene that has been centrifuged at 500 revolutions per minute. The line slightly above the bottom line is for 1000 rpm and the graph line at the top represents the absorbance for sample centrifuged at 1500 rpm Graphene.

As we can see the absorbance values increase as we increase rpm of centrifugation.

The small peak in the middle of each curve, at around 550 nm, shows that we are moving from UV to Visible region.

- **Tungsten Disulfide, WS_2**

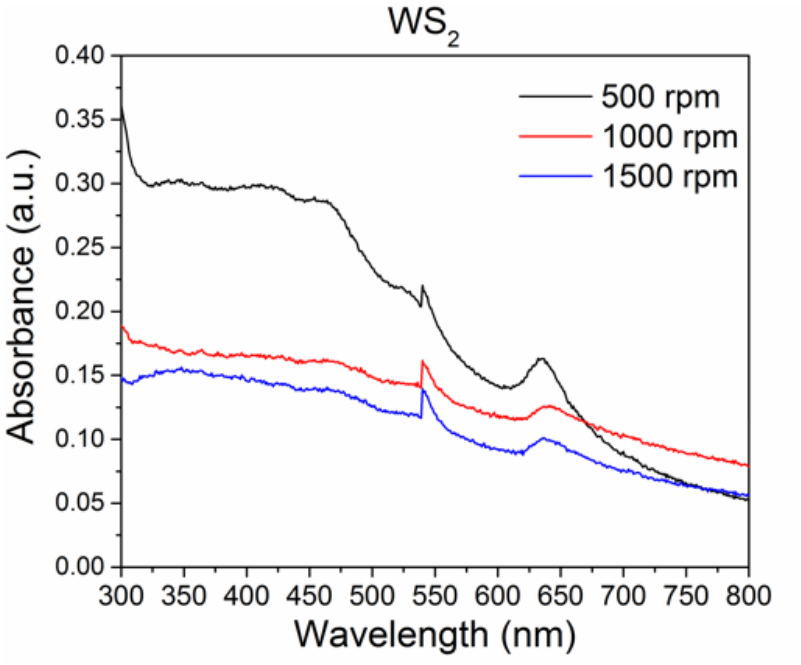

The graphs obtained for the UV-Vis of Tungsten Disulfide, WS_2.

Peak at the top is for WS2 at 500 rpm, Peak in the middle is for WS2 at 1000 rpm, and peak at the bottom indicates WS2 sheets at 1500 rpm. We can see that absorbance values for each wavelength value decrease as we increase rpm of centrifugation, from 500 to 1000 to 1500 this is due to the fact that by increased rpm, size of nanosheets is reduce so absorbance value is reduced.

The peaks in the middle, at around 550 nm, again show that the wavelength is going from the UV region into the visible region.

5.5Electrochemical workstation

In order to calculate the electrochemical properties of the WS_2, Gr exfoliated and separated at 1500, 1000, 500 rpm and WS_2Gr composites which is Layer by Layer (LBL) assembly of nanosheets on the PET films, the cyclic voltammetry (CV) and galvanostatic charge/discharge tests were performed on Electrochemical Deposition Workstation.

The CV curves for the Graphene, WS_2 and WS_2Gr composites electrodes at a scanning rate of 100 mVs^{-1} in the potential window of -0.3 to 0.7 V which is over the 1 V in 1 M Na2SO4 electrolyte are shown in the graphs.

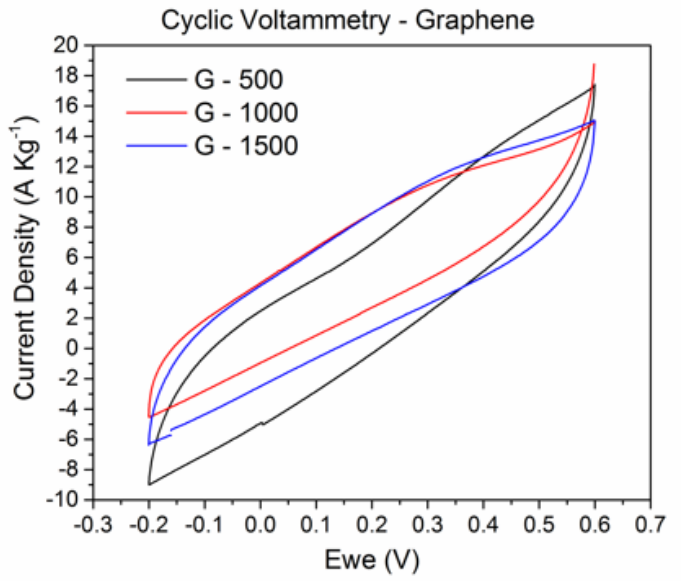

Fig. The CV curves for the Graphene (1500, 1000, 500) electrodes.

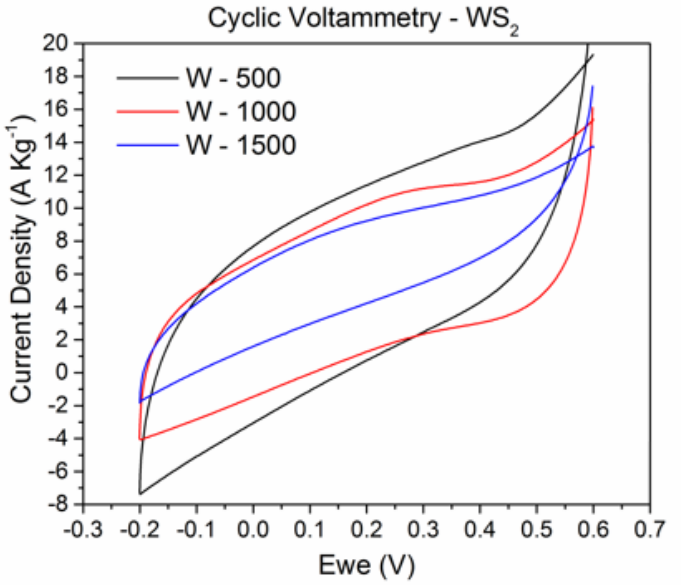

Fig. The CV curves for the WS_2 (1500, 1000, 500) electrodes.

It can be observed that, the area of the Cyclic Voltammetry curve for the WS2/Gr electrode is larger than the WS_2 and Gr electrodes individually, this larger area of

curve also indicates higher specific capacitance and the synergistic effect of WS_2 and Gr combined.

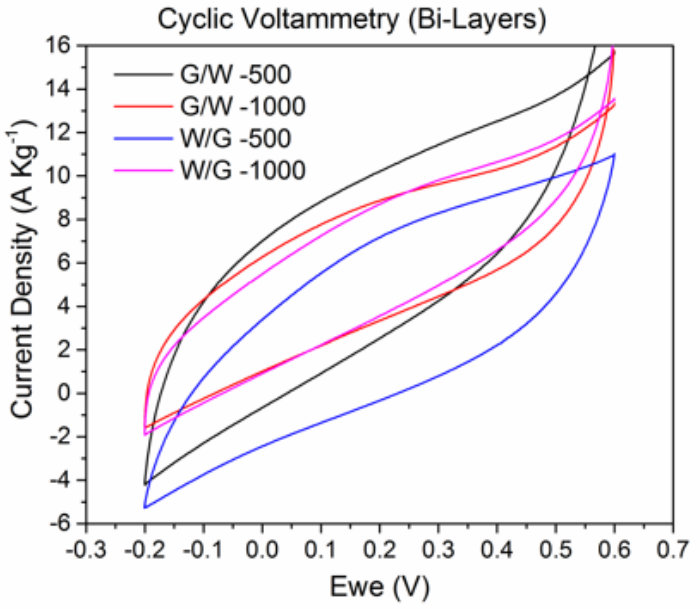

Fig. The large area CV curves for the G/WS_2 (500, 1000) and WS_2/G (500, 1000), Bi-layer composite electrodes.

To further explore the properties of the WS_2 and Gr composites electrode, The Cyclic Voltammetry tests are being done on different assembly designs at various scan rates from 10 to 100 mVs^{-1} to exhibit quasi-rectangular shapes which is clear evidence that all the samples have a good capacitive behavior.

The CV curves obtained at fast scan rates have larger area than curves at lower scan rate one, but it does not represent the large charge capacitance at the higher scan rates. Meanwhile, It is clear that by increasing the scan rate, the effective interaction between the ions and the electrode is reduced considering the fact that the resistance of metal oxide and the deviance from rectangularity of the CV curves becomes obviously.

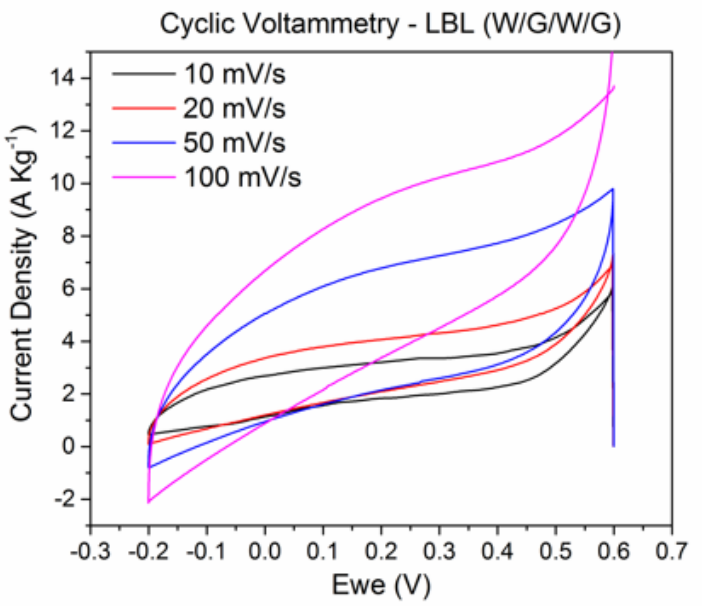

Fig. The CV curves for the WS_2/G/WS_2/G (1000, 500) layer by layer assembled composite electrodes at scanning rates of 100, 50, 20, 10 mVs^{-1}.

The constant current charge/discharge curves of WS_2 /Gr composites at current densities (-2, 4, 10, and 16 A/kg). During the charge/discharge steps, the charge curve of Bi-layer composites is almost symmetric to its discharge counterpart with very low internal resistance (IR) drop, which indicates the pseudo-capacitive contributions with the Bi-layer contribution.

The specific capacitance (Csp) of the electrode is obtained from the following equation:

$$\mathbf{Csp = A / (v*m)}$$

where A, v, m are the constant current (A), discharge time (s), the total potential difference (V) and the weight of active materials (kg), respectively.

The specific capacitance of W/G/W/G 500rpm composites remain as high as 246.4997 F kg^{-1} and for G/W/G/W 500rpm it is 125 F kg^{-1} ,even at a high discharge current densities. These results indicate that the W/G/W/G composites have a high rate of capacitance due to the graphene layer being on the top, which is recognized

as one of the most important material for electrochemical properties in the application of electrodes and batteries.

The variation of the specific capacitance (farad per unit mass) with the different lateral size is shown in graph. The higher the lateral dimensions higher will be the specific capacitance. Nanosheets centrifuged at 1500 rpm have small lateral size dimensions that is why those sheets have very small value of specific capacitance. On the other hand samples centrifuged at 500 rpm have very large lateral dimensions that why they possess very high specific capacitance. Samples for 1000rpm have intermediate specific capacitance.

The advantages of WS_2 /Gr composites over the WS_2, Gr electrodes are significant and the exceptional electrochemical performances of WS_2/Gr composites are due to their unique structure:

1. Layered WS_2 sheets on the surfaces of Gr nanosheets gather to formulate pores for ion-buffering reservoir to improve the ionic diffusion rate.
2. The nanoscale size of WS_2 and large specific surface area of the WS_2/Gr composites significantly reduce the diffusion length of both ions and electrons transfer during the charging and discharging process. This speeds up utilization of the electrode, that is nanoscale size of WS_2 sheets;
3. Gr acts as supports in the composites for the filling of WS_2 sheets, but also constructs a 3-D model of highly conductive current collector.
4. The excellent interfacial contact of WS_2 and Gr assists fast transference of electrons throughout the electrode matrix. This unique architecture enables the WS_2/Gr composites electrode to possess a large specific surface and fast ionic and electronic transportation.

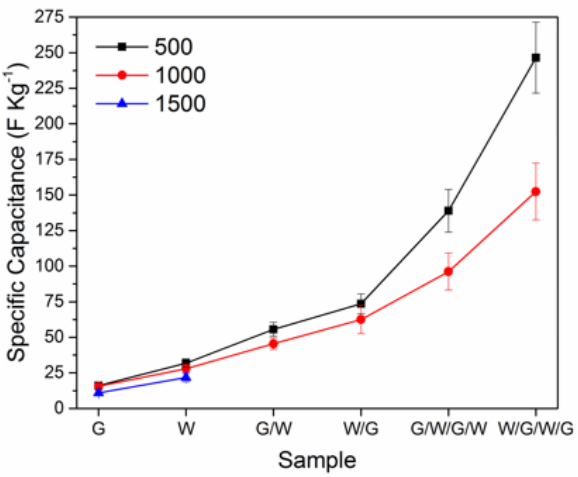

Fig. The variation of the specific capacitance (farad per unit mass) for G, WS_2, G/W, W/G, G/W/G/W and W/G/W/G for layers separated at 500, 1000, 1500rpm is shown in graph.

From the graph it can be observed that WS_2/G composites have much higher specific capacitance as compare to G and WS_2 separately.

Table. Specific Capacitance.

Samples	***Specific Capacitance* (F kg^{-1})**
G 500	*15.97444*
W 500	*31.84713*
G/W 500	*52.63159*
W/G 500	*71.42875*
G/W/G/W 500	*125*
W/G/W/G 500	*246.4997*
G-1000	*16.58375*
W- 1000	*27.93296*
G/W 1000	*35.71428*
W/G 1000	*28.46153*
G/W/G/W 1000	*104.16667*
W/G/W/G 1000	*127.55102*

G 1500	*13.609145*
W- 1500	*19.23076*

The energy and power densities can be derived from galvanostatic charging and discharging sequence at various current densities. The specific energy density (E) and the power density (P) are evaluated by equations:

$$E = 1/2CV^2$$

$$P = E/Dt$$

In above equations C is the capacitance, V is the voltage decrease by discharging, E is the energy and Dt is the time taken to discharge.

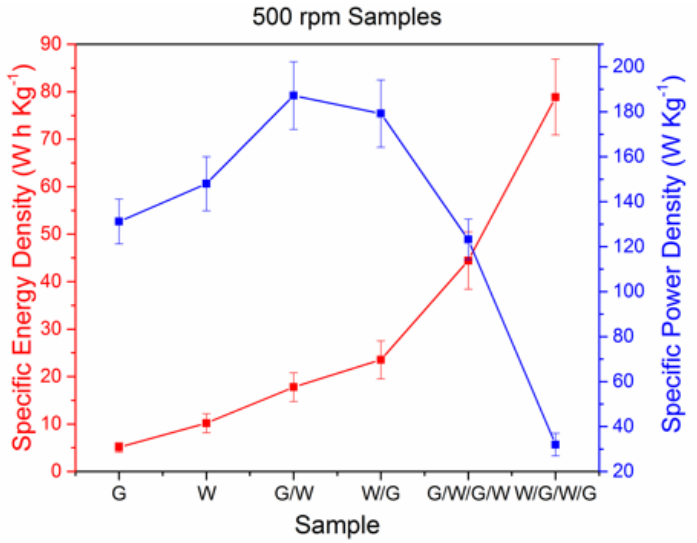

Graph: Specific Energy Density and Specific Power Density of 500 rpm samples of graphene and WS_2 and W/G composites.

As seen from the graphs, as the power density increases from 131.2 W kg^{-1} for Gr separated at 500 rpm to 187.2 W kg^{-1} Gr/W for 500 rpms. The energy density of Gr also increased from 5.11 W h kg^{-1} to 78.88 W h kg^{-1}, and the power densities of composites then start decreasing with increased specific energy densities.

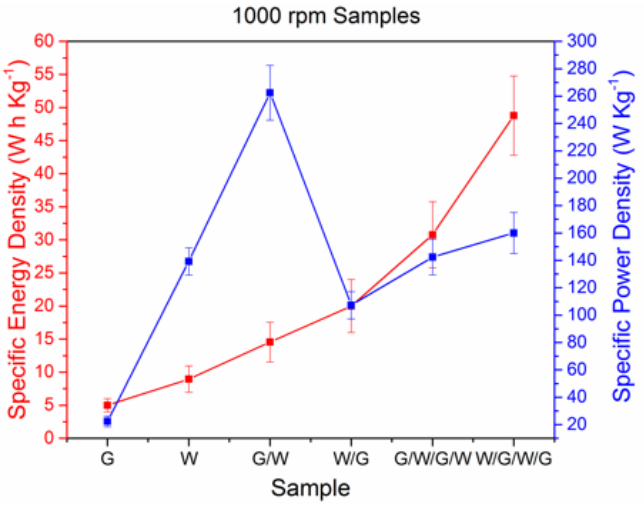

Graph: Specific Energy Density and Specific Power Density of 1000 rpm samples of graphene and WS_2 and W/G composites.

Table: Specific Energy Density and Specific Power Density of G, W and their composites at 500, 1000, 1500 rpms

Samples	***Specific Energy Density (W kg^{-1})***	***Specific Power Density (W h kg^{-1})***
G 500	5.111821	131.2
W 500	10.19108	128
G/W 500	16.84	187.2
W/G 500	22.8571	179.2
G/W/G/W 500	40	123.2
W/G/W/G 500	78.87991	32
G-1000	5.306799	22.4
W- 1000	8.938547	139.2
G/W 1000	11.482	462.4
W/G 1000	12.3076	107.2
G/W/G/W 1000	33.34	142.4
W/G/W/G 1000	40.81629	160
G 1500	4.35496	193.6
W- 1500	6.13568	155.2

Comparatively, the energy density of the WS_2/Gr composites can reach 32 W kg^{-1} at a power density of 78.9 W h kg^{-1}. This exhibited a very large power density that can be obtained while maintaining a high energy density.

The results clearly indicates that the WS_2/G composites electrode materials have excellent electrochemical properties possessing high energy density and power output.

The cycle stability of W/G composites was evaluated by repeated current charging and discharging tests between the voltage range of -0.3 and +0.7 V at a current density of 1.0 A kg^{-1} for 1000 cycles.

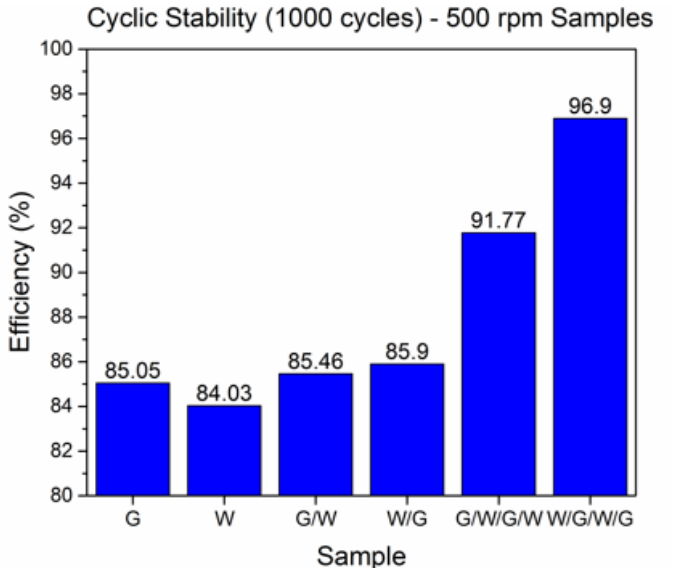

Graph: G, W and G/W composites cyclic stability in % efficiency for nanosheets separated at 500 rpm.

From graph, The capacitance only decreases by about 14.5.% for Graphene electrode at 500 rpm. 15.93% for WS_2 electrode at 500 rpm, which is maximum decrease in capacitance of the initial capacitance after 1000 cycles.

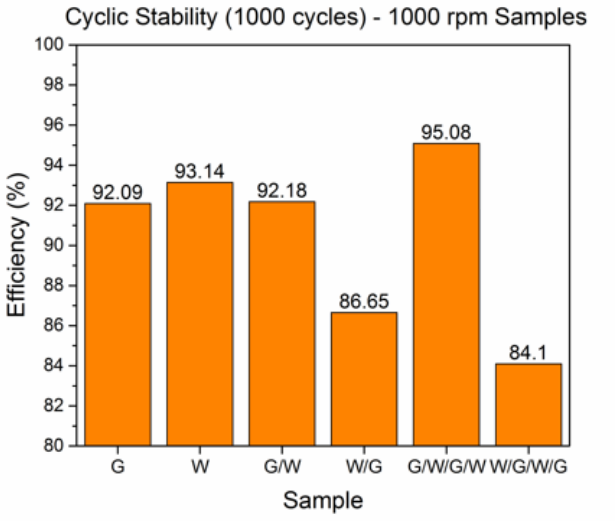

Graph: G, W and G/W composites cyclic stability in % efficiency for nanosheets separated at 1000 rpm.

Maximum efficiency achieved for W/G/W/G is about 96.9 % indicating a good cycling life of the composites materials and its use in commercial super capacitors.

Therefore, an increased capacitance and retention displayed in these tests are attributed to the flexibility of Graphene in the composites. The Graphene can not only form an open assembly to improve the linking between the active material e.g. WS_2 and electrolyte Na_2SO_4 and the full use of PET conductive film during the charge and discharge processes, but also increase of electrical conductivity of the electrode because of the high conductivity of Graphene.

➢ Conclusion

We synthesized 2D nanosheets of Graphene and Tungsten Disulfide (WS_2) for different lateral dimensions and made G/WS_2 composites with alternate stacking of nanosheets in known quantity to make heterogeneous structures. Electrochemical properties of these materials were improved by varying assembly design and concentration of 1M Na_2SO_4.

The maximum specific capacitance achieved from **W/G/W/G (at 500 rpm)** is 246F kg^{-1} at a charge/discharge current density 50 A kg^{-1} compared to 127.6 F kg^{-1} for **G/W/G/W (at 1000 rpm)** composite. For WS_2 and Gr at 1000 rpm was 27.9 F kg^{-1} and 16.6 F kg^{-1} and for 500 rpm it was 31.8 F kg^{-1} and 15.9 F kg^{-1} respectively.

The integration of Graphene (Conductor) into the composites with WS_2 (Semiconductor) provides relatively large areas to loading WS_2 sheets, leading to heterogeneous nanostructures. Thus WS_2Gr composites enable an easy access to charge-transfer and ion transport through the electrode. Furthermore, the capacitance retention is still over 96% of initial capacitance after 1000 cycles. These results suggest that the WS_2Gr composites are quite a suitable and favorable

electrode material for high performance energy storage devices like supercapacitors.

➢ Future Work:

The scope is very bright. In electronic system, wearable electronics, Electronic Vehicles, as also medical implants, supercapacitors are coming up with solutions which could not be thought of earlier. Robots, UAV will find use of supercapacitors due to quick charging capacity.

In power for vehicles, already buses, trams and trains have started running on supercapacitors. Trains are also making use of Kinetic Energy Recovery Systems (KERS) and saving huge amount of energy. As energy density increases, cars may also start being powered by them. Presently many functions are being increasingly taken over by supercapacitors in vehicles, helping increase battery life also in the process.

Graphene with other materials demonstrate marvelous properties. So, our future work is on how to effectively make a junction of these materials, to crop more surprising properties for the energy storage.

In future, if supercapacitors were used in electric vehicles (EVs) as the primary energy storage, then it can be fully recharge in less than 5-seconds to go for up to 300 miles. However, that would require very large conductors to transfer the electrons to the supercapacitors (ohmic heating issues) to cope with this issue different assembly design of composites would be needed so that we can further increase the charge storage density. So, a 5-minute charge is could be affordable in hardware and reasonable in charging time.

Supercapacitors do not have the wear-n-tear of ions running back and forth, which causes various build-up of materials (dendrites) that impede ion movement or

reduce active sites. That is why it is relatively easy to improve the life-cycle over 500,000 to over 1-million with highest possible % efficiency. Future supercapacitors will be in the 250-400 W h/kg range, which means most EVs will have the majority of the energy storage in supercapacitors and probably less than 10-20% in Li-ion cells.

So the overall the future for supercapacitors is quite bright yet challenging.

References:

1. John, B., and Bates, *THIN FILM BATTERY.* United States Patent, Patent no. 5338625, 1994.
2. Philipp Adelhelm, P.H., Conrad L Bender, Martin Busche, Christine Eufinger, and Juergen Janek, *From lithium to sodium: cell chemistry of room temperature sodium–air and sodium–sulfur batteries.* Beilstein J Nanotechnol, 2015.
3. Shaheen, S., Ginley, D., & Jabbour, G., *Organic-Based Photovoltaics: Toward Low-Cost Power Generation.* MRS Bulletin, 2005. **30**(1).
4. Dunn, B., H. Kamath, and J.-M. Tarascon, *Electrical Energy Storage for the Grid: A Battery of Choices.* Science, 2011. **334**(6058): p. 928-935.
5. Simon, P., Y. Gogotsi, and B. Dunn, *Where Do Batteries End and Supercapacitors Begin?* Science, 2014. **343**(6176): p. 1210-1211.
6. F. Croce, A.D.E., J. Hassoun, A. Deptula, T.Olczac, and B.Scrosati, *A Novel Concept for the Synthesis of an Improved LiFePO4 Lithium Battery Cathode.* Electrochemical an Solid-State letters, 2002. **5**(3).
7. Sarangapani, S., *Materials for Electrochemical Capacitors,Theoretical and Experimental Consfraints.* 1995.
8. Pandolfo, A.G. and A.F. Hollenkamp, *Carbon properties and their role in supercapacitors.* Journal of Power Sources, 2006. **157**(1): p. 11-27.
9. Mai, L.-Q., et al., *Hierarchical MnMoO4/CoMoO4 heterostructured nanowires with enhanced supercapacitor performance.* Nature Communications, 2011. **2**: p. 381.
10. Pokropivny, V.V. and V.V. Skorokhod, *Classification of nanostructures by dimensionality and concept of surface forms engineering in nanomaterial science.* Materials Science and Engineering: C, 2007. **27**(5): p. 990-993.
11. Cheng, L., et al., *PEGylated WS2 Nanosheets as a Multifunctional Theranostic Agent for in vivo Dual-Modal CT/Photoacoustic Imaging Guided Photothermal Therapy.* Advanced Materials, 2014. **26**(12): p. 1886-1893.

12. Cong, C., et al., *Synthesis and Optical Properties of Large-Area Single-Crystalline 2D Semiconductor WS2 Monolayer from Chemical Vapor Deposition.* Advanced Optical Materials, 2014. **2**(2): p. 131-136.
13. Zhang, Y., et al., *Controlled Growth of High-Quality Monolayer WS2 Layers on Sapphire and Imaging Its Grain Boundary.* ACS Nano, 2013. **7**(10): p. 8963-8971.
14. Zhang, H., *Ultrathin two-dimensional nanomaterials.* ACS nano, 2015. **9**(10): p. 9451-9469.
15. Yu, X., et al., *Emergent Pseudocapacitance of 2D Nanomaterials.* Advanced Energy Materials: p. 1702930-n/a.
16. Lee, T., et al., *Layer-by-Layer Assembly for Graphene-Based Multilayer Nanocomposites: Synthesis and Applications.* Chemistry of Materials, 2015. **27**(11): p. 3785-3796.
17. Dong, X., et al., *Layer-by-Layer Engineered Co–Al Hydroxide Nanosheets/Graphene Multilayer Films as Flexible Electrode for Supercapacitor.* Langmuir, 2012. **28**(1): p. 293-298.
18. Brent, J.R., N. Savjani, and P. O'Brien, *Synthetic approaches to two-dimensional transition metal dichalcogenide nanosheets.* Progress in Materials Science, 2017. **89**: p. 411-478.